Photon transport in a one-dimensional nanophotonic waveguide QED system

2016 Phys. Scr. 91 063004

(http://iopscience.iop.org/1402-4896/91/6/063004)

IOP Publishing | Royal Swedish Academy of Sciences Physica Scripta

Phys. Scr. **91** (2016) 063004 (16pp) doi:10.1088/0031-8949/91/6/063004

Invited Comment

Photon transport in a one-dimensional nanophotonic waveguide QED system

Zeyang Liao[1], Xiaodong Zeng[1], Hyunchul Nha[2] and M Suhail Zubairy[1]

[1] Institute for Quantum Science and Engineering (IQSE) and Department of Physics and Astronomy, Texas A&M University, College Station, TX 77843-4242, USA
[2] Department of Physics, Texas A&M University at Qatar, Education City, PO Box 23874, Doha, Qatar

E-mail: zeyangliao@physics.tamu.edu and zubairy@physics.tamu.edu

Received 19 January 2016, revised 14 March 2016
Accepted for publication 12 April 2016
Published 9 May 2016

Abstract

The waveguide quantum electrodynamics (QED) system may have important applications in quantum device and quantum information technology. In this article we review the methods being proposed to calculate photon transport in a one-dimensional (1D) waveguide coupled to quantum emitters. We first introduce the Bethe ansatz approach and the input–output formalism to calculate the stationary results of a single photon transport. Then we present a dynamical time-dependent theory to calculate the real-time evolution of the waveguide QED system. In the longtime limit, both the stationary theory and the dynamical calculation give the same results. Finally, we also briefly discuss the calculations of the multiphoton transport problems.

Keywords: photon transport, waveguide QED, nanophotonics

(Some figures may appear in colour only in the online journal)

1. Introduction

Since photons are ideal carriers for quantum information, manipulating and routing photons can have important applications in the quantum information technology and quantum device [1–7]. However, the photons in the vacuum rarely interact with each other and it is difficult to manipulate the photons without resort to the photon–atom interaction. Nevertheless, the photon–atom coupling in the vacuum is usually very weak. Fortunately, this coupling strength can be enhanced by modifying the environment by the Purcell effect [8]. For instance, strong photon–atom interaction can be achieved by confining the photon in a cavity [9–11] or reduced dimension structures such as in one-dimensional (1D) or quasi-1D photonic waveguide with transverse cross sections being of the order of a wavelength square [12–14]. Recently, photon transport in a 1D or quasi-1D photonic waveguide system coupled to quantum emitters, which is termed as 'waveguide quantum electrodynamics (QED)', has been widely studied both in theory [15–58] and experiment [59–70]. This waveguide QED system is very interesting because the waveguide system can not only enhance the coupling strength between the photon and the emitter, but also guide the photons which is good for quantum information transport [71]. Both of which are important properties for quantum information technology and quantum device applications. There are a number of systems that can act as a quasi-1D waveguide such as optical nanofibers [59], photonic crystal with line defects [72], surface plasmon nanowire [61], and superconducting microwave transmission lines [73–77].

A single photon scattered by a single emitter embedded in a 1D waveguide has been studied by Shen and Fan [15, 16]. They employed the real space description of the Dicke Hamiltonian and the Bethe-ansatz approach to derive the stationary transport properties of the photon transport. It is shown that a photon with frequency resonant to the two-level quantum emitter can be completely reflected due to quantum interference [15]. Since then, several alternative methods have been proposed to calculate the photon transport in a waveguide QED system such as the method based on Lippmann–Schwinger scattering theory [34, 78] and the method based on the input–output theory [37, 38]. An extension of the

stationary theory was developed by Rephaeli *et al* to derive the perfect inverting pulse where they project the initial quantum state to the stationary eigenstates of the system and then apply a time evolution operator [23]. In 2011, Chen *et al* illustrated a time-dependent theory to calculate a single photon transport in 1D waveguide coupled to a single emitter where they can calculate the real-time evolution of the single photon pulse and the dynamics of the emitter [24]. For an infinitely long 1D waveguide, the maximum excitation of the emitter by a photon being incident from one direction is 50%. However, for a semi-infinite 1D waveguide the maximum excitation of an emitter can be larger than 50% [23, 24, 49]. Photon transport in a quasi-1D waveguide with finite cross section coupled to a single emitter has also been studied [34, 36].

Compared with the single emitter case, a single photon transport in a 1D waveguide coupled to multiple emitters is more interesting because more physics may emerge due to the collective interactions between the emitters. The collective spontaneous emission by an ensemble of identical atoms has been extensively studied since the pioneering work of Dicke in 1954 [79–88]. Due to the collective interaction, the decay rate can be significantly enhanced or suppressed, and the emission spectrum can also be significantly altered [89–91]. The spontaneous emission from a pair of two-level atoms near a nanofiber has been studied where a substantial radiative exchange is predicted between distant atoms [92]. The stationary calculation of a single photon scattered by multiple emitters coupled to a 1D waveguide has also been studied where it is shown that the transmission spectrum can be strongly modified [25, 26]. In 2015, we extended the method shown in [24] and derive a time-dependent dynamical theory for this collective many-body system which allows us to study the real time evolution of the photon transport and atomic excitations [58]. We show that, due to the collective interaction, the reflectivity of a single-photon pulse with finite bandwidth can approach 100%. Many interesting physical phenomena can occur in this system such as the photonic bandgap effects [15], long-range quantum entanglement generation [93, 94], Fano-like interference [95–98], and superradiant effects [82].

In addition to the single photon transport, multiple-photon transport is also very interesting because creating strong photon-photon interaction at a few-photon level plays a critical role in the quantum information technology. Few-photon scattering by a quantum emitter coupled to a 1D waveguide has been studied by the Bethe ansatz approach [17, 40, 56], Lehmann–Symanzik–Zimmermann reduction approach [41], and the input–output theory [37]. It is found that the photons can strongly interact with each other and they can exchange the momentum. More interestingly, photon bound state can occur due to the interaction between the photons and the quantum emitters [17, 31]. General formalism for multiple photons interact with an atomic system has also been considered based on the property of integrability [56], diagrammatic method [57], input–output formalism [42] and master equation approach [43].

The calculations of photon transport in a 1D waveguide coupled to a multi-level quantum emitter or an optical cavity have also been studied. In these systems, electromagnetic induced transparency [18] and photon blockade effects [44] may be observed. In addition, a single-photon diode [47, 52], efficient single-photon frequency conversion [20, 46, 48, 50], and single-photon transistor [4, 35, 99] may also be realized. A single-photon quantum router with multiple output ports [54] and two-photon control phase gate in a 1D waveguide QED system [32, 39] have been proposed as well. Thus, the studying of waveguide QED system is very interesting and useful.

This article is organized as follows. In section 3 we show the calculation of single photon transport in a 1D waveguide coupled to a quantum emitter. In this section, we first show the stationary calculations based on Bethe ansatz approach and the input–output formalism. Then we discuss the dynamical solutions. In section 4, we show the calculation of single photon transport in a 1D waveguide coupled to multiple quantum emitters. We also discuss the results based on the Bathe ansatz approach and the dynamical solution. In section 5, we show the calculation of few-photon transport in a 1D waveguide coupled to a single quantum emitters based on Bethe ansatz approach and the input–output formalism. In section 6, we briefly discuss the calculation of multiple photons interacting with a local atomic system coupled to 1D waveguide. The last section is the summary and outlook.

2. Model and Hamiltonian

In this article, we show the calculations of how a single or a few photons transport through a 1D waveguide coupled to one or multiple quantum emitters. We mainly consider four cases: (1) a single photon interacts with a single quantum emitter (figure 1(a)); (2) a single photon interacts with a quantum emitter array (figure 1(b)); (3) a few photons interact with a single quantum emitter (figure 1(c)); (4) a few photons interact with a system of quantum emitters (figure 1(d)). Here, we mainly focus on the case that the quantum emitters are two-level systems which are coupled to a 1D single mode waveguide. The quantum emitters can be atoms, quantum dots, superconducting qubits and so on. The Hamiltonian of the system in the rotating wave approximation is given by [58, 79, 100]

$$H = \frac{\hbar}{2}\left(\omega_{\mathrm{a}} - \mathrm{i}\frac{\gamma}{2}\right)\sum_{j=1}^{N_{\mathrm{a}}}\sigma_j^z + \hbar\sum_k \omega_k a_k^\dagger a_k + \hbar\sum_{j=1}^{N_{\mathrm{a}}}\sum_k (g_k^j a_k \sigma_j^+ + g_k^{j*} a_k^\dagger \sigma_j^-), \quad (1)$$

where the first term is the atomic energy including the spontaneous decay to the non-guided modes, the second term is the energy of the guided photon modes, and the third term is the coupling between the atoms and the guided photon modes. Here we would mention that we just add a phenomenological decay rate γ for the effect of the non-

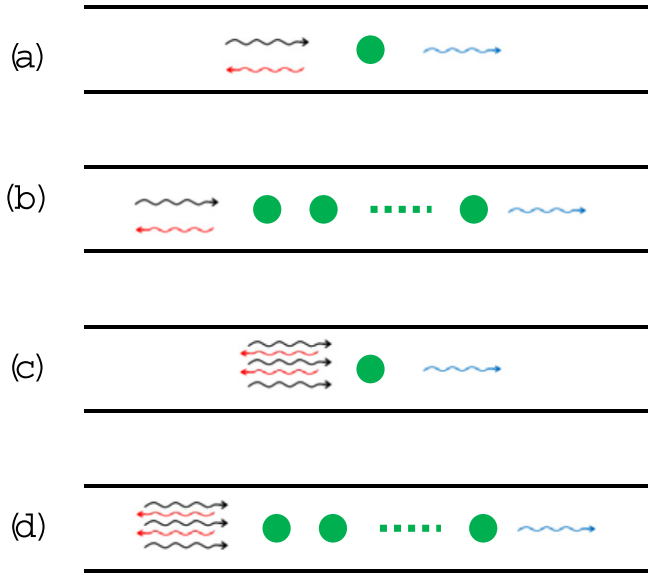

Figure 1. The models to be studied in this article. (a) Single photon transport in a 1D waveguide coupled with single quantum emitter. (b) Single photon transport in a 1D waveguide coupled with multiple quantum emitters. (c) Few-photon transport in a 1D waveguide with single quantum emitter. (d) Few-photon transport in a 1D waveguide with multiple quantum emitters.

guided vacuum modes because we would mainly focus on the atom and the guided photon space. This is valid whenever the atomic separation is not too small compared with the wavelength resonant to the two-level atom. If the atomic separation is much smaller than the wavelength resonant to the two-level atom, the interaction between the atomic system and the free-space vacuum modes can induce a strong dipole-dipole interacton and cause a significant energy shift which can not be neglected. However, this is out of the scope of this article, and we would just add a phenomenological decay rate in equation (1) to include the effect of the non-guided vacuum modes. In equation (1), ω_a is the transition frequency of the two-level emitters, ω_k is the angular frequency of the photon with wavevector k, γ is the spontaneous decay rate due to the non-guided modes, $\sigma_j^+ = |e\rangle_j\langle g|(\sigma_j^- = |g\rangle_j\langle e|)$ is the raising (lowering) operator of the jth atom, and $a_k^\dagger(a_k)$ is the creation (annihilation) operator of the guided photon with wavevector k, $g_k^j = (\boldsymbol{\mu}\cdot\mathbf{E}_k(r_j))/\hbar$ is the coupling strength between the jth emitter and the guided photon mode with wavevector k, where $\boldsymbol{\mu}$ is the transition dipole moment of the emitter and $\mathbf{E}_k(r_i)$ is the electric field strength of mode k at position r_j.

The typical photonic dispersion curve of a single mode waveguide is shown in figure 2 [27]. Assume that ω_a is far away from the cutoff frequency of the photonic waveguide and the guided photon has a narrow bandwidth. The dispersion relation for the guided photon can be approximately linearized as

$$\omega_k = \omega_a + (|k| - k_a)v_g, \tag{2}$$

where k_a is the wavevector at frequency ω_a and v_g is the group velocity [27]. Therefore, for the right propagating modes, we have $\omega_k = \omega_a + (k - k_a)v_g$ with $k > 0$, and for the left propagating modes, we have $\omega_k = \omega_a + (-k - k_a)v_g$ for $k < 0$. The calculations in the following sections are based on the Hamiltonian shown in equation (1) and the linearized dispersion relation shown in equation (2).

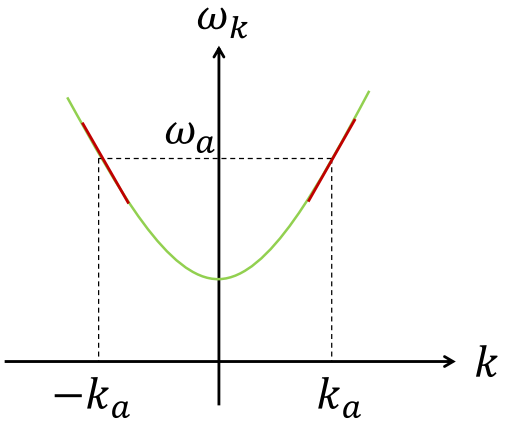

Figure 2. Typical photonic dispersion of a single mode waveguide and the linearization around the atomic frequency. Reproduced with permission from [27]. Copyright American Physical Society 2009.

3. Single photon scattered by single emitter

Let us first look at the simplest case where a single photon is scattered by a single emitter. In this case, the Hamiltonian is given by

$$H = \frac{\hbar}{2}\left(\omega_a - i\frac{\gamma}{2}\right)\sigma^z + \hbar\sum_k \omega_k a_k^\dagger a_k + \hbar g\sum_k (a_k\sigma^+ + a_k^\dagger\sigma^-). \tag{3}$$

In the following subsections, we first illustrate the static solution based on Bethe ansatz approach and the input–output formalism. Then we show a dynamical time-dependent solution of this system.

3.1. Static solution: Bethe ansatz approach

In the 1D waveguide, the photon mode can be decomposed as left and right propagating modes [15, 27], i.e.

$$\sum_k \omega_k a_k^\dagger a_k = \sum_{k_R}\omega_{k_R} a_{k_R}^\dagger a_{k_R} + \sum_{k_L}\omega_{k_L} a_{k_L}^\dagger a_{k_L}, \tag{4}$$

where $a_{k_R}^\dagger$ (a_{k_R}) creates (annihilates) a right-propagating photon and $a_{k_L}^\dagger$ (a_{k_L}) creates (annihilates) a left-propagating photon. By performing the Fourier transformations $a_{k_R} = \int_{-\infty}^{\infty} a_R(x)e^{ik_R x}dx$, $a_{k_R}^\dagger = \int_{-\infty}^{\infty} a_R^\dagger(x)e^{-ik_R x}dx$, where $a_R^\dagger(x)$ ($a_R(x)$) creates (annihilates) a right-propagating photon and similar transformations for the left-propagating photon, the Hamiltonian in equation (3) can be rewritten in the real

space as [15, 27]

$$H = \left(\omega_a - i\frac{\gamma}{2}\right)|e\rangle\langle e| + \int dx\,[a_R^\dagger(x)(\omega_a - iv_g\partial_x)a_R(x) + a_L^\dagger(x)(\omega_a + iv_g\partial_x)a_L(x)] + g\int dx\delta(x)[a_R^\dagger(x)\sigma^- + a_R(x)\sigma^+ + a_L^\dagger(x)\sigma^- + a_L(x)\sigma^+], \tag{5}$$

where we have set $\hbar = 1$.

Assume that a single photon is indent from the left with photon energy given by $\omega_k = \omega_a + \delta k v_g$. The stationary state of the system can be expressed as [15]

$$|E_k\rangle = \int dx\,[\phi_{k,R}(x)a_R^\dagger(x) + \phi_{k,L}(x)a_L^\dagger(x)]|g, 0\rangle + e_k|e, 0\rangle, \tag{6}$$

where $|g, 0\rangle$ is the state with zero photon and the emitter being in the ground state and $|e, 0\rangle$ is the state when the emitter is excited and no photon in waveguide. $\phi_{k,R}(x)$ is the amplitude that a right-propagating photon is generating at position x, $\phi_{k,L}(x)$ is the amplitude that a left-propagating photon is generating at position x, and e_k is the probability amplitude of the emitter being excited. From the eigen-equation $H|E_k\rangle = \hbar\omega_k|E_k\rangle$ and using the following ansatz:

$$\phi_{k,R}(x) = e^{ikx}[\theta(-x) + t\theta(x)], \tag{7}$$

$$\phi_{k,L}(x) = re^{-ikx}\theta(-x), \tag{8}$$

where t is the transmission coefficient, r is the reflection coefficient, and $\theta(x)$ is a step function with $\theta(x) = 1$ if $x > 0$ and $\theta(x) = 0$ if $x < 0$, one can obtain the following equations

$$\left(\delta k v_g + i\frac{\gamma}{2}\right)e_k = g(1 + r), \tag{9}$$

$$iv_g(1 - t) = ge_k, \tag{10}$$

$$iv_g r = ge_k. \tag{11}$$

The solutions of these equations are given by

$$e_k = \frac{g}{\delta k v_g + i\left(\frac{g^2}{v_g} + \frac{\gamma}{2}\right)}, \tag{12}$$

$$r = \frac{\frac{g^2}{v_g}}{-\left(\frac{g^2}{v_g} + \frac{\gamma}{2}\right) + i\delta k v_g}, \tag{13}$$

$$t = \frac{-\frac{\gamma}{2} + i\delta k v_g}{-\left(\frac{g^2}{v_g} + \frac{\gamma}{2}\right) + i\delta k v_g}. \tag{14}$$

The reflectivity and transmissivity are then given by

$$R = \frac{\Gamma^2}{(\Gamma + \gamma)^2 + (2\delta k v_g)^2}, \tag{15}$$

$$T = \frac{\gamma^2 + 4\delta k^2 v_g^2}{(\Gamma + \gamma)^2 + (2\delta k v_g)^2}, \tag{16}$$

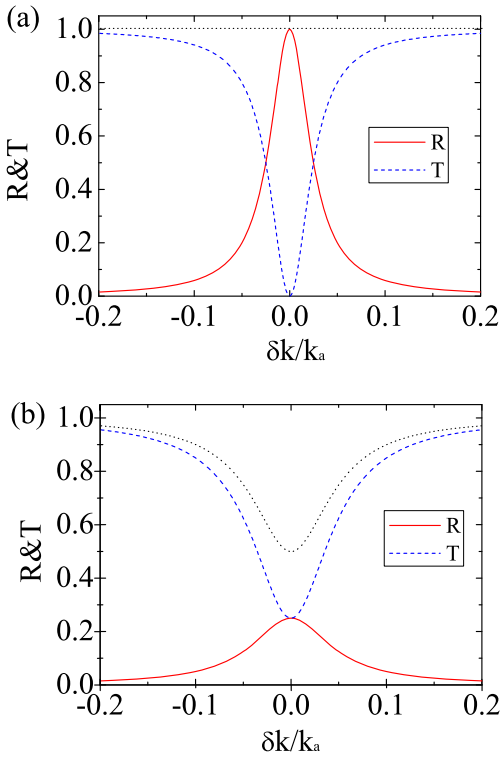

Figure 3. The reflection (red solid curve) and transmission (blue dashed curve) spectrum with $\Gamma = 0.05k_a v_g$. The black dotted curve is the summation of the reflection and transmission. (a) $\gamma = 0$; (b) $\gamma = \Gamma$.

where $\Gamma = 2g^2/v_g$ is the decay rate due to coupling between the quantum emitter and the waveguide modes. It is readily noted that if $\delta k = 0$ and neglecting the decay to the nonguided modes ($\gamma = 0$), we have $R = 1$ and $T = 0$, i.e., the resonant frequency component is completely reflected back [15]. This is due to the destructive quantum interference between the incoming photon filed and the reemited photon field by the quantum emitter [58].

Typical reflection and transmission spectrum are shown in figure 3(a) where we assume the decay to the nonguided modes is zero (i.e., $\gamma = 0$). Again we see that the resonant frequency is completely reflected back and the frequency away from the resonant frequency can transmit. However, when the decay to the non-guided modes is included, the resonant frequency has certain probability to be transmitted (figure 3(b)). This is because the perfect quantum interference between the incoming photon field and the reemited photon field has been destroyed. We should also note that the total energy of guided modes, especially frequencies around the resonant frequency, has been significantly reduced due to the emission to the free space (see the dotted line in figure 3(b)).

An alternative way to calculate the static reflection and transmission spectrum is by the Lippmann–Schwinger approach. For details, please see the [34].

3.2. Scattering matrix: input–output formalism

In this subsection, we illustrate how to calculate the scattering matrix for single photon scattered by a single emitter in a 1D

waveguide based on the input–output formalism [37, 101, 102]. A scattering process can be well characterized by a scattering matrix and its elements are defined as [41]

$$_{\text{out}}\langle f|\text{i}\rangle_{\text{in}} =_{\text{in}} \langle f|S|\text{i}\rangle_{\text{in}}, \tag{17}$$

where the scattering matrix S is given by

$$S = T\exp\left[-\text{i}\int_{-\infty}^{+\infty} H_{\text{int}}\,\text{d}t\right] \tag{18}$$

with T being the time-ordering operator and H_{int} being the interaction between the photons and the quantum emitters.

Here it is easier to work in the frequency domain. The Hamiltonian in equation (3) can be rewritten as [37]

$$H = \frac{1}{2}\left(\omega_{\text{a}} - \text{i}\frac{\gamma}{2}\right)\sigma^{z} + \int_{-\infty}^{\infty}\omega a_{\omega}^{\dagger}a_{\omega} + \frac{g}{v_{\text{g}}}\int_{-\infty}^{\infty}\text{d}\omega\,(a_{\omega}\sigma^{+} + a_{\omega}^{\dagger}\sigma^{-}), \tag{19}$$

where $a_{\omega} = a_{k}/\sqrt{v_{\text{g}}}$ which satisfies $[a_{\omega}, a_{\omega'}^{\dagger}] = \delta(\omega - \omega')$ and we set $\hbar = 1$. To simplify the notation, in this subsection we denote ω_k and ω_p as $\tilde{k}$ and $\tilde{p}$, respectively.

For a single photon transport, the scattering matrix is defined by $S_{\tilde{p},\tilde{k}} =_{\text{out}} \langle\tilde{p}|\tilde{k}\rangle_{\text{in}}$, where $|\tilde{p}\rangle_{\text{out}} = a_{\text{out}}^{\dagger}(\tilde{p})|0\rangle$ is a state after the scattering with frequency $\tilde{p}$ and $|\tilde{k}\rangle_{\text{in}} = a_{\text{in}}^{\dagger}(\tilde{k})|0\rangle$ is a state before the scattering with frequency $\tilde{k}$. We then have

$$S_{\tilde{p},\tilde{k}} = \langle 0|a_{\text{out}}(\tilde{p})a_{\text{in}}^{\dagger}(\tilde{k})|0\rangle = \frac{1}{2\pi}\int_{-\infty}^{\infty}\text{d}t\,\langle 0|a_{\text{out}}(t)|\tilde{k}^{-}\rangle\text{e}^{\text{i}\tilde{p}t} \tag{20}$$

in which $|\tilde{k}^{-}\rangle = a_{\text{in}}^{\dagger}(\tilde{k})|0\rangle$ is the input state with frequency $\tilde{k}$, and '-' ('+') denotes the distant past (future). In the second identity of the equation, we use the Fourier transformation

$$a_{\text{out}}(\tilde{p}) = \frac{1}{2\pi}\int_{-\infty}^{\infty}\text{d}t a_{\text{out}}(t)\text{e}^{\text{i}\tilde{p}t}. \tag{21}$$

Therefore, to calculate the scattering matrix we need to first calculate $\langle 0|a_{\text{out}}(t)|\tilde{k}^{-}\rangle$ which can be evaluated by the Heisenberg equations.

From the Heisenberg equations with the Hamiltonian shown in equation (19), we can obtain [37]

$$\frac{\text{d}\sigma^{-}(t)}{\text{d}t} = -\text{i}\left(\omega_{\text{a}} - \text{i}\frac{\gamma}{2}\right)\sigma^{-}(t) + \text{i}\sqrt{\Gamma}\,\sigma^{z}(t)a_{\text{in}}(t) - \frac{\Gamma}{2}\sigma^{-}(t), \tag{22}$$

$$a_{\text{out}}(t) = a_{\text{in}}(t) - \text{i}\sqrt{\Gamma}\,\sigma^{-}(t) \tag{23}$$

in which $\Gamma = 2\pi g^{2}/v_{\text{g}}$ and we have used the following transformations

$$a_{\text{in}}(t) = \frac{1}{\sqrt{2\pi}}\int\text{d}\tilde{k}a_{\tilde{k}}(t_0)\text{e}^{-\text{i}\tilde{k}(t-t_0)}, \tag{24}$$

$$a_{\text{out}}(t) = \frac{1}{\sqrt{2\pi}}\int\text{d}\tilde{k}a_{\tilde{k}}(t_1)\text{e}^{-\text{i}\tilde{k}(t-t_1)} \tag{25}$$

with $t_0 \to -\infty$ and $t_1 \to +\infty$.

By inserting $\langle 0|$ and $|\tilde{k}^{-}\rangle$ on both sides of equations (22) and (23) we can obtain

$$\frac{\text{d}}{\text{d}t}\langle 0|\sigma^{-}|\tilde{k}^{-}\rangle = -\left(\text{i}\omega_{\text{a}} + \frac{\Gamma+\gamma}{2}\right)\langle 0|\sigma^{-}(t)|\tilde{k}^{-}\rangle + \text{i}\sqrt{\Gamma}\,\langle 0|\sigma^{z}(t)a_{\text{in}}(t)|\tilde{k}^{-}\rangle, \tag{26}$$

$$\langle 0|a_{\text{out}}(t)|\tilde{k}^{-}\rangle = \langle 0|a_{\text{in}}(t)|\tilde{k}^{-}\rangle - \text{i}\sqrt{\Gamma}\,\langle 0|\sigma^{-}(t)|\tilde{k}^{-}\rangle. \tag{27}$$

The second term of the right-hand side of equation (26) can be calculated by

$$\langle 0|\sigma^{z}(t)a_{\text{in}}(t)|\tilde{k}^{-}\rangle = -\langle 0|a_{\text{in}}(t)a_{\text{in}}^{\dagger}(\tilde{k})|0\rangle = \frac{1}{2\pi}\text{e}^{-\text{i}\tilde{k}t}, \tag{28}$$

where we have use the Fourier transformation of $a_{\text{in}}(t)$ which is given by

$$a_{\text{in}}(t) = \frac{1}{2\pi}\int_{-\infty}^{\infty}\text{d}\tilde{k}a_{\text{in}}(\tilde{k})\text{e}^{-\text{i}\tilde{k}t}. \tag{29}$$

Inserting equations (28) into (26) we can solve

$$\langle 0|\sigma_{-}|\tilde{k}^{-}\rangle = \frac{1}{\sqrt{2\pi}}\text{e}^{-\text{i}\tilde{k}t}s_{\tilde{k}} \tag{30}$$

with

$$s_{\tilde{k}} = \frac{2\sqrt{\Gamma}}{2(\tilde{k}-\omega_{\text{a}}) + \text{i}(\Gamma+\gamma)}. \tag{31}$$

Plugging equations (30) into (27), one can get

$$\langle 0|a_{\text{out}}(t)|\tilde{k}^{-}\rangle = \frac{1}{\sqrt{2\pi}}\text{e}^{-\text{i}\tilde{k}t}t_{\tilde{k}} \tag{32}$$

with

$$t_{\tilde{k}} = \frac{2(\tilde{k}-\omega_{\text{a}}) - \text{i}(\Gamma-\gamma)}{2(\tilde{k}-\omega_{\text{a}}) + \text{i}(\Gamma+\gamma)}. \tag{33}$$

After Fourier transformation, we get the scattering matrix given by

$$S_{\tilde{p},\tilde{k}} = t_{\tilde{k}}\delta(\omega_k - \omega_p). \tag{34}$$

From $t_{\tilde{k}}$ we can get the reflection and transmission coefficients which are respectively given by

$$R_{\tilde{k}} = \left|\frac{t_{\tilde{k}}-1}{2}\right|^{2} = \frac{\Gamma^{2}}{4\delta k^{2}v_{\text{g}}^{2} + (\Gamma+\gamma)^{2}}, \tag{35}$$

$$T_{\tilde{k}} = \left|\frac{t_{\tilde{k}}+1}{2}\right|^{2} = \frac{4\delta k^{2}v_{\text{g}}^{2} + \gamma^{2}}{4\delta k^{2}v_{\text{g}}^{2} + (\Gamma+\gamma)^{2}}, \tag{36}$$

where $\delta k v_{\text{g}} = \tilde{k} - \omega_{\text{a}}$. The results are consistent with previous calculation based on the Bethe ansatz approach [15, 27].

3.3. Dynamical solution

In the real case, the photon is always a pulse instead of a plane wave and one may also be interested in the real-time evolution of the quantum emitter. In this subsection, we derive a dynamical equation for a single photon propagates through 1D waveguide coupled to a two-level quantum emitter. For a single photon excitation, the quantum state of

the system at arbitrary time can be expressed as [24, 58]

$$|\Psi(t)\rangle = \alpha_1(t)\mathrm{e}^{-\mathrm{i}\omega_a t}|e, 0\rangle + \sum_k \beta_k(t)\mathrm{e}^{-\mathrm{i}\omega_k t}|g, 1_k\rangle, \quad (37)$$

where $|e, 0\rangle$ is the state with the atom being in the ground state and zero photon in the waveguide, $|g, 1_k\rangle$ is the state with the atom being in the ground state and one photon with wavevector k being in the waveguide.

From the Schrödinger equation $\mathrm{i}\partial_t|\Psi(t)\rangle = H|\Psi(t)\rangle$ with the Hamiltonian shown in equation (3), the dynamics of the system is given by

$$\dot{\alpha}_1(t) = -\mathrm{i}g\sum_k g_k \mathrm{e}^{\mathrm{i}kr_1}\beta_k(t)\mathrm{e}^{-\mathrm{i}\delta\omega_k t} - \frac{\gamma}{2}\alpha_1(t), \quad (38)$$

$$\dot{\beta}_k(t) = -ig^*\mathrm{e}^{-\mathrm{i}kr_1}\alpha_1(t)\mathrm{e}^{\mathrm{i}\delta\omega_k t}, \quad (39)$$

where r_1 is the position of the quantum emitter and $\delta\omega_k \equiv \omega_k - \omega_a = (|k| - k_a)v_g$ is the detuning between the atomic transition frequency and the frequency of the guided photon.

By integrating equation (39) one obtains

$$\beta_k(t) = \beta_k(0) - \mathrm{i}g^*\mathrm{e}^{-\mathrm{i}kr_1}\int_0^t \alpha_1(t')\mathrm{e}^{\mathrm{i}\delta\omega_k t'}\mathrm{d}t', \quad (40)$$

where $\beta_k(0)$ is the initial photon amplitude. On substituting equations (40) into (38) one can get the dynamic of the emitter excitation

$$\dot{\alpha}_1(t) = -\mathrm{i}g\sum_k \mathrm{e}^{\mathrm{i}kr_j}\beta_k(0)\mathrm{e}^{-\mathrm{i}\delta\omega_k t} - \frac{\gamma}{2}\alpha_1(t) - |g|^2\sum_k\int_0^\infty \alpha_1(t')\mathrm{e}^{\mathrm{i}\delta\omega_k t'}\mathrm{d}t'\mathrm{e}^{-\mathrm{i}\delta\omega_k t}. \quad (41)$$

For a long 1D waveguide we can replace the summation over k by integration $\sum_k \to (L/2\pi)\int_{-\infty}^{\infty}\mathrm{d}k$ with L being the quantization length in the 1D waveguide. On summing over k and integrating over t', equation (41) becomes

$$\dot{\alpha}_1(t) = -\frac{\mathrm{i}}{2\pi}\sqrt{\frac{\Gamma v_g L}{2}}\int_{-\infty}^{\infty}\beta_k(0)\mathrm{e}^{\mathrm{i}kr_1 - \mathrm{i}\delta\omega_k t}\mathrm{d}k - \frac{\Gamma+\gamma}{2}\alpha_1(t), \quad (42)$$

where $\Gamma = 2L|g_{k_a}|^2/v_g$ is the decay rate due to the coupling between the atom and the waveguide photon modes. Given the initial conditions and equation (42), one can calculate the emitter excitations at an arbitrary time.

Assume that the atoms are initially in the ground state and the input single photon pulse has a Gaussian shape given by $\beta_{\delta k}(0) = (8\pi/\sqrt{\Delta L})^{1/4}\mathrm{e}^{-\frac{\delta k^2}{\Delta^2}}$ with the full width at half maximum of the spectrum being $\sqrt{2\ln 2}\,\Delta v_g$ [104]. Here a single photon number requires $(L/2\pi)\int_{-\infty}^{\infty}\|\beta_{\delta k}(0)\|^2\mathrm{d}\delta k = 1$. We should mention that this method can be used to calculate the transport of a single photon with arbitrary pulse shape.

The formal solution of equation (42) can be written as [24, 58]

$$\alpha_1(t) = -\mathrm{i}S\{\mathrm{erf}(C + \sqrt{B}\,t_0) - \mathrm{erf}(C)\}\mathrm{e}^{-\frac{\Gamma+\gamma}{2}t}, \quad (43)$$

where $C = (A - 2Bt_0)/2\sqrt{B}$ with $t_0 = r_1/v_g$, $A = -(\Gamma+\gamma)/2$, and $B = \Delta^2 v_g^2/4$. $S = (\pi/8)^{1/4}\sqrt{(\Gamma+\gamma)/\Delta v_g}\,\mathrm{e}^{-At_0 + A^2/4B}\mathrm{e}^{\mathrm{i}k_a r_1}$, and $\mathrm{erf}(x) = (2/\sqrt{\pi})\int_0^x \mathrm{e}^{-t^2}\mathrm{d}t$ is the error function. The emitter excitation as a function of time with $\Gamma = \Delta v_g$ is shown as the black solid line in figure 4(a). We see that when the photon pulse propagates through the quantum emitter the atom is first excited and then deexcited. The maximum value of excitation for the Gaussian input in this example is about 40% which is close to the 50% limit. The 50% limit can be explained by the following reason: since the photon pulse incident from one direction can be decomposed as odd and even modes and only even mode can couple to the emitter, the maximum excitation by a photon incident from one direction is 50%. The 50% limit can be reached by the inversion pulse incident from one side as discussed in [23] (see the red dotted line in figure 4(a)).

After obtaining the quantum emitter excitation $\alpha_1(t)$, one can also calculate the real-time evolution of the photon spectrum from equation (40). The reflected and transmitted spectra can be also calculated by setting $t \to \infty$. Supposing that the input photon is incident from the left, the transmitted spectrum is given by

$$\beta_{\delta k}^{\mathrm{R}} = \beta_k(0) - \mathrm{i}\sqrt{\frac{\Gamma v_g}{2L}}\mathrm{e}^{-\mathrm{i}(k_a+\delta k)r_1}\chi_1(\delta k), \quad (44)$$

where $\delta k = k - k_a$ with $k > 0$. The reflection spectrum is given by

$$\beta_{\delta k}^{\mathrm{L}} = -\mathrm{i}\sqrt{\frac{\Gamma v_g}{2L}}\mathrm{e}^{\mathrm{i}(k_a+\delta k)r_1}\chi_1(\delta k), \quad (45)$$

where $\delta k = |k| - k_a$ with $k < 0$ and $\chi_1(\delta k)$ is the Fourier transformation of $\alpha_1(t)$ given by

$$\chi_1(\delta k) = \int_{-\infty}^{\infty}\alpha_1(t)\mathrm{e}^{\mathrm{i}\delta k v_g t}\mathrm{d}t, \quad (46)$$

where $\alpha_1(t) = 0$ when $t < 0$. By performing the inverse Fourier transformation we have

$$\alpha_1(t) = \frac{v_g}{2\pi}\int_{-\infty}^{\infty}\chi_1(\delta k)\mathrm{e}^{-\mathrm{i}\delta k v_g t}\mathrm{d}\delta k. \quad (47)$$

Inserting equations (47) into (42) yields

$$-\mathrm{i}\delta k v_g\chi_1(\delta k) = b_1(\delta k) - \frac{\Gamma+\gamma}{2}\chi_1(\delta k) \quad (48)$$

with $b_1(\delta k) = -\mathrm{i}\sqrt{\Gamma L/2v_g}\,\beta_{\delta k}(0)\mathrm{e}^{\mathrm{i}(k_a+\delta k)r_1}$ being the input spectrum.

It is readily to obtain the solution of equation (48) which is

$$\chi_1(\delta k) = -\mathrm{i}\sqrt{\frac{\Gamma L}{2v_g}}\mathrm{e}^{\mathrm{i}(k_a+\delta k)r_1}\frac{\beta_{\delta k}(0)}{\frac{\Gamma+\gamma}{2} - \mathrm{i}\delta k v_g}. \quad (49)$$

The photon spectra after the interaction can then be calculated from equations (44) and (45) and given by

$$\beta_{\delta k}^{\mathrm{R}} = -\frac{(2\mathrm{i}\delta k v_g)\beta_{\delta k}(0)}{(\Gamma+\gamma)^2 - 2\mathrm{i}\delta k v_g}, \quad (50)$$

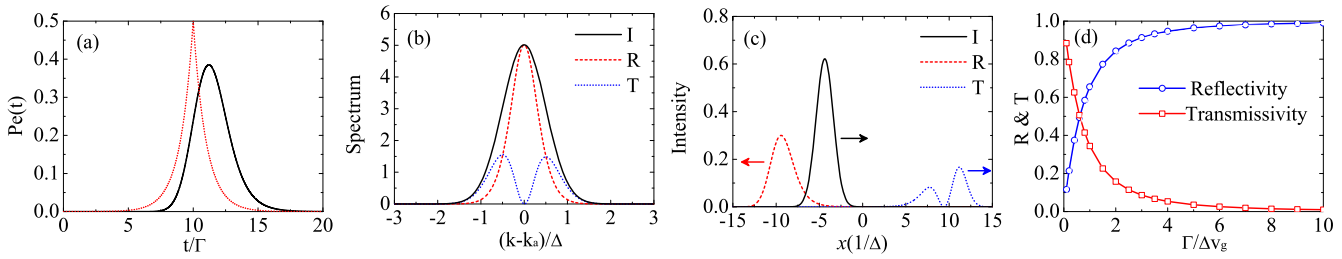

Figure 4. (a) The emitter excitation as a function time with the black solid curve being the result for the Gaussian input while the red dotted curve being the result for the inversion pulse given by [23]. (b) The spectra of the incoming, reflected and transmitted photon. (c) The pulse shapes of the incoming, reflected and transmitted photon. (d) The reflectivity and transmissivity as a function of coupling strength over the photonic bandwidth. Here, *I* is incoming; *R* is reflection; *T* is transmission. Parameters: $\Gamma = \Delta v_g$. Figure reprinted with permission from Liao *et al* (2015) [58]. Copyright 2015 by the American Physical Society.

$$\beta_{\delta k}^{L} = -e^{2i(k_a+\delta k)r_1}\frac{\Gamma\beta_{\delta k}(0)}{(\Gamma+\gamma)-2i\delta k v_g}, \tag{51}$$

with $\beta_{\delta k}(0)$ being the initial photon wavepacket.

The reflectivity and transmissivity for each frequency component are given by

$$R = \frac{\Gamma^2}{(\Gamma+\gamma)^2+4\delta k^2 v_g^2}, \tag{52}$$

$$T = \frac{4\delta k^2 v_g^2}{(\Gamma+\gamma)^2+4\delta k^2 v_g^2} \tag{53}$$

which is consistent with the static solution calculated by the Bethe ansatz and the input–output formalism shown in the previous subsections. Again, when $\delta k = 0$ and $\gamma = 0$, we have $R = 1$, i.e., the resonant component is completely reflected. It is also noted that $R + T = 1$ when $\gamma = 0$, which means that the mode is conserved.

The spectra of the photon before and after the interaction with $\Gamma = \Delta v_g$ are shown in figure 4(b). The spectrum of the reflected photon is similar to but narrower than that of the input photon. The bandwidth of the reflected photon can be controlled by changing the coupling strength. Nevertheless, the transmitted spectrum is quite different where there are two peaks. In current example, the reflectivity of the photon pulse is about 66% with the resonant frequency component being completely reflected.

The photon pulse shape in arbitrary time can be calculated by performing the Fourier transformations of the photon spectra. The typical reflected and transmitted photon pulse shapes are shown in figure 4(c) with the black solid curve being the incoming photon pulse, the red dotted curve being the reflected photon pulse, and the blue dashed curve being the transmitted photon pulse. The reflected pulse shape is similar to the incoming pulse shape, but with a reduced amplitude. On the contrary, the transmitted pulse shape is quite different where there are two peaks due to the interference between the incoming photon field and the reemitted photon field.

For a photon pulse with finite bandwidth, the total reflectivity and transmissivity can be calculated by summing over all the frequency components. The total reflectivity for a Gaussian input pulse is given by

$$R = \sqrt{\frac{\pi}{2}}\int_{-\infty}^{\infty}\frac{e^{-2y^2}}{1+4y^2/\eta^2}dy \tag{54}$$

and the transmissivity $T = 1 - R$ where $\eta = \Gamma/\Delta v_g$. It is noted that the reflectivity and transmissivity of a single emitter system depends only on the ratio $\Gamma/\Delta v_g$. When $\eta \to 0$, $R \to 0$ and $T \to 1$, which means that the photon can not be reflected without coupling. When $\eta \to \infty$, $R \to 1$ and $T \to 0$, i.e, the photon can be completely reflected if the coupling strength is very large comparing with the photon bandwidth. The reflectivity and transmissivity, as a function of $\Gamma/\Delta v_g$, are shown in figure 4(d). The reflectivity increases when $\Gamma/\Delta v_g$ increases and it can approach 100% when $\Gamma/\Delta v_g \gg 1$. Similar to the reflectivity, the reflection bandwidth also increases by increasing the ratio $\Gamma/\Delta v_g$ (see the green line with triangle symbol in figure 4(d)).

4. Single photon scattered by multiple emitters

Generalization from single emitter to multiple emitters is straightforward, but it is not trivial because the collective interaction between the emitters may strongly modify the dynamics and the spectrum of the system. In this section, we first illustrate the calculation by the Bethe ansatz approach [25] and then we discuss the dynamical solution [58].

4.1. Static solution: Bethe ansatz approach

For simplicity, here we neglect the decay to the non-guided modes (i.e., $\gamma = 0$). The Hamiltonian for the multiple-emitter system with $\gamma = 0$ can be written as [25]

$$\begin{aligned} H = {} & \omega_a\sum_{j=1}^{N}|e\rangle_j\langle e| + \int dx\,[a_R^\dagger(x)\left(\omega_a - iv_g\frac{\partial}{\partial x}\right)a_R(x) \\ & + a_L^\dagger(x)\left(\omega_a + iv_g\frac{\partial}{\partial x}\right)a_L(x)] + g\sum_{j=1}^{N}[a_R^\dagger(x_j)\sigma_j^- \\ & + a_R(x_j)\sigma_j^+ + a_L^\dagger(x_j)\sigma_j^- + a_L(x_j)\sigma_j^+]. \end{aligned} \tag{55}$$

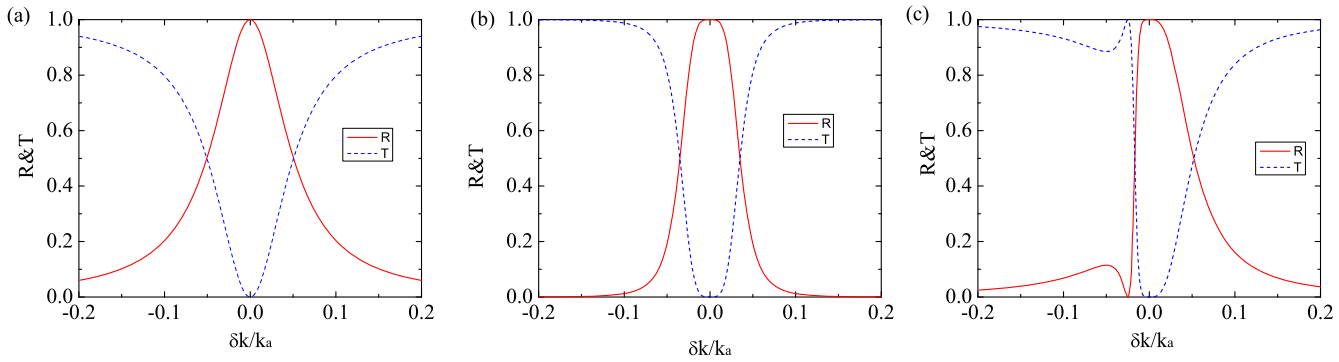

Figure 5. The reflection and transmission spectra when there are two emitters. (a) $a = \lambda/2$; (b) $a = \lambda/4$; (c) $a = \lambda/8$. Parameters: $\Gamma = 0.05k_a v_g$.

Similar to the one-emitter case, the eigenvectors of the system can be expressed as

$$|E_k\rangle = \int \mathrm{d}x\,[\phi_k^{\mathrm{R}}(x)a_{\mathrm{R}}^{\dagger}(x) + \phi_k^{\mathrm{L}}(x)a_{\mathrm{L}}^{\dagger}(x)]|g,\,0\rangle + \sum_{j=1}^{N} e_k^j|e_j,\,0\rangle, \tag{56}$$

where $|g,\,0\rangle$ is the vacuum state with all the atoms being in the ground state and $|e_j,\,0\rangle$ is the vacuum state with the jth atom being in the excited state and all other atoms being in the ground state. $\phi_{k,\mathrm{R}}(x)$ is the amplitude that a right-propagating photon is generating at position x, $\phi_{k,\mathrm{L}}(x)$ is the amplitude that a left-propagating photon is generating at position x, and e_k^j is the probability amplitude that the jth emitter is excited.

From the eigen-equation $H|E_k\rangle = \hbar\omega_k|E_k\rangle$ and using the following ansatz:

$$\phi_k^{\mathrm{R}}(x) = \begin{cases} \mathrm{e}^{\mathrm{i}kx} & x < 0, \\ t_j\mathrm{e}^{\mathrm{i}k(x-ja)} & (j-1)a < x < ja, \\ t_N\mathrm{e}^{\mathrm{i}k(x-Na)} & x > (N-1)a \end{cases}$$

and

$$\phi_k^{\mathrm{L}}(x) = \begin{cases} r_1\mathrm{e}^{-\mathrm{i}kx} & x < 0, \\ r_{j+1}\mathrm{e}^{-\mathrm{i}k(x-ja)} & (j-1)a < x < ja, \\ 0 & x > (N-1)a \end{cases}$$

with a being the atomic separation, r_j and t_j being coefficients to be determined, one can obtain the following relations [25]

$$\begin{bmatrix} t_j \\ r_{j+1} \end{bmatrix} = M^j \begin{bmatrix} 1 \\ r_1 \end{bmatrix} \tag{57}$$

with $j = 1, 2, \ldots, N$ and $r_{N+1} = 0$. Here $M = PQ$, where

$$P = \begin{bmatrix} \mathrm{e}^{\mathrm{i}ka} & 0 \\ 0 & \mathrm{e}^{-\mathrm{i}ka} \end{bmatrix}$$

and

$$Q = \begin{bmatrix} 1 - \mathrm{i}\frac{\Gamma}{2\delta k v_g} & -\mathrm{i}\frac{\Gamma}{2\delta k v_g} \\ \mathrm{i}\frac{\Gamma}{2\delta k v_g} & 1 + \mathrm{i}\frac{\Gamma}{2\delta k v_g} \end{bmatrix}$$

with $\Gamma = 2g^2/v_g$.

From equation (57), it is straightforward to obtain

$$r_1 = -\frac{(M^N)_{21}}{(M^N)_{22}}, \tag{58}$$

$$t_N = (M^N)_{11} - \frac{(M^N)_{12}(M^N)_{21}}{(M^N)_{22}} \tag{59}$$

where M^N can be calculated as [106]

$$M^N = \frac{1}{\sin\beta}[M\sin N\beta - I\sin(N-1)\beta] \tag{60}$$

with the angle β satisfying $\cos\beta = \cos ka + (\Gamma/2\delta k v_g)\sin ka$. From equations (58) to (60) one notes that the transmission is maximum when $\sin N\beta = 0$ which corresponds to $\beta = j\pi/N$ with $j = 1, 2, \ldots, N-1$. For $\delta k \ll k_a$, the transmission peaks occur at around

$$\delta k_j \simeq \frac{\frac{\Gamma}{2v_g}\sin(k_a a)}{\cos(j\pi/N) - \cos(k_a a)}. \tag{61}$$

Take the two-emitter system as an example. From equations (58) and (59) with $N = 2$, one can obtain

$$r_1 = \frac{(1 + \mathrm{e}^{2\mathrm{i}ka})(1 - 2\mathrm{i}\delta k v_g/\Gamma) - 2\mathrm{e}^{2\mathrm{i}ka}}{(1 - 2\mathrm{i}\delta k v_g/\Gamma)^2 - \mathrm{e}^{2\mathrm{i}ka}}, \tag{62}$$

$$t_2 = \frac{-4\delta k^2 v_g^2/\Gamma^2}{(1 - 2\mathrm{i}\delta k v_g/\Gamma)^2 - \mathrm{e}^{2\mathrm{i}ka}} \tag{63}$$

and the reflectivity and transmissivity are given by $|r_1|^2$ and $|t_2|^2$ respectively. The reflection and transmission spectra for three emitter separations are shown in figure 5. When $a = \lambda/2$, the spectrum are similar to the one emitter case with the resonant frequency being completely reflected. When $a = \lambda/4$, there is a bandwidth of frequency around the resonant frequency that has very low transmissivity, which is similar to the photonic bandgap effect. When $a = \lambda/8$, the spectra are quite different where both the reflection and transmission spectra are asymmetric. The transmission spectrum has a peak at position $\Gamma/2v_g$ which can be calculated from equation (61).

For the results when $N > 2$, please refer to [25].

4.2. Dynamical solution

For a single photon interacting with an atomic chain coupled to a 1D waveguide, the Hamiltonian is given by equation (1). The quantum state of the system in an arbitrary time can be expressed as

$$|\Psi(t)\rangle = \sum_{j=1}^{N_a}\alpha_j(t)e^{-i\omega_a t}|e_j, 0\rangle + \sum_k \beta_k(t)e^{-i\omega_k t}|g, 1_k\rangle, \quad (64)$$

where $|e_j, 0\rangle$ is the state where only the jth atom is in the excited state with zero photon in the waveguide, and $|g, 1_k\rangle$ is the state where all the atoms are in the ground state with one photon with wavevector k being in the waveguide.

Following the procedures shown in section 3.3, we can obtain the dynamic equation of the emitters given by [58]

$$\dot{\alpha}_j(t) = b_j(t) - \sum_{l=1}^{N_a}\left(\frac{\Gamma}{2}e^{ik_a r_{jl}} + \frac{\gamma}{2}\delta_{jl}\right)\alpha_l\left(t - \frac{r_{jl}}{v_g}\right), \quad (65)$$

with

$$b_j(t) = -\frac{i}{2\pi}\sqrt{\frac{\Gamma v_g L}{2}}\int_{-\infty}^{\infty}\beta_k(0)e^{ikr_j - i\delta\omega_k t}dk, \quad (66)$$

$\Gamma = 2L|g_{k_a}|^2/v_g$ being the effective coupling strength and $r_{jl} = |r_j - r_l|$. The second term is the collective interaction between the quantum emitters mediated by the guided photon modes. Different from the free space, the collective interactions induced by the guided photon is a long-range effect. Thus, nearest-neighbor approximation is invalid in 1D waveguide system. We also note that there is a time-retarded effect for the collective interactions. When the separations between the emitters are small, this time-retarded effect may be neglected which is the usual Markov approximation. The real parts of the collective interaction terms are the collective damping while the imaginary parts shift the energies of the collective eigenstates. Given the initial conditions, we can calculate the emitter excitations in an arbitrary time from equation (72) by the numerical methods such as finite-difference time-domain method [103].

The photon spectrum in arbitrary time can also be calculated. Supposing that the photon is incident from the left, the spectrum of the right propagating mode at time t is given by

$$\beta_{\delta k}^{R}(t) = \beta_k(0) - i\sqrt{\frac{\Gamma v_g}{2L}}\sum_{j=1}^{N_a}e^{-i(k_a+\delta k)r_j}\int_0^t \alpha_j(t')e^{i\delta k v_g t'}dt', \quad (67)$$

where $\delta k = k - k_a$ with $k > 0$. The spectrum of the left propagating mode is given by

$$\beta_{\delta k}^{L}(t) = -i\sqrt{\frac{\Gamma v_g}{2L}}\sum_{j=1}^{N_a}e^{i(k_a+\delta k)r_j}\int_0^t \alpha_j(t')e^{i\delta k v_g t'}dt'. \quad (68)$$

where $\delta k = |k| - k_a$ with $k < 0$.

To calculate the photon spectrum when $t \to \infty$, we can perform similar Fourier transformation as in section 3.3 and obtain a set of linear equations which are given by

$$-i\delta k v_g \chi_j(\delta k) = b_j(\delta k) - \frac{\gamma}{2}\chi_j(\delta k) + \sum_{l=1}^{N_a}V_{N_a}^{jl}(\delta k)\chi_l(\delta k), \quad (69)$$

where $\chi_j(\delta k) = \int_{-\infty}^{\infty}\alpha_j(t)e^{i\delta k v_g t}dt$, $b_j(\delta k) = -i\sqrt{\Gamma L/2v_g}\beta_{\delta k}(0)e^{i(k_a+\delta k)r_j}$ and the collective coupling matrix V_{N_a} is given by

$$V_{N_a}(\delta k) = -\frac{\Gamma}{2}\begin{bmatrix} 1 & e^{ika} & \cdots & e^{i(N_a-1)ka} \\ e^{ika} & 1 & \cdots & e^{i(N_a-2)ka} \\ \vdots & \vdots & \ddots & \vdots \\ e^{i(N_a-1)ka} & e^{i(N_a-2)ka} & \cdots & 1 \end{bmatrix} \quad (70)$$

with $k = k_a + \delta k$.

From equation (69), we can determine

$$\chi_j(\delta k) = \sum_{l=1}^{N_a}M_{jl}^{-1}(\delta k)b_l(\delta k), \quad (71)$$

where $M(\delta k) = -V_{N_a}(\delta k) + (\gamma/2 - i\delta k v_g)I_{N_a}$ with I_{N_a} being a $N_a \times N_a$ unit matrix. The photon spectra for the right and left propagating photon at $t \to \infty$ are respectively given by

$$\beta_{\delta k}^{R}(t \to \infty) = \beta_{\delta k}(0) - i\sqrt{\frac{\Gamma v_g}{2L}}\sum_{j=1}^{N_a}e^{-i(k_a+\delta k)r_j}\chi_j(\delta k), \quad (72)$$

$$\beta_{\delta k}^{L}(t \to \infty) = -i\sqrt{\frac{\Gamma v_g}{2L}}\sum_{j=1}^{N_a}e^{i(k_a+\delta k)r_j}\chi_j(\delta k). \quad (73)$$

Given the photon spectrum, one can easily obtain the photon pulse in real space by simply performing the Fourier transformation.

Let us take two-atom system as an example. From equation (65), the emitter excitation dynamics for two-emitter system can be written as

$$\begin{bmatrix}\dot{\alpha}_1(t) \\ \dot{\alpha}_2(t)\end{bmatrix} = \begin{bmatrix}b_1(t) \\ b_2(t)\end{bmatrix} + V_2(0)\begin{bmatrix}\alpha_1\left(t - \frac{a}{v_g}\right) \\ \alpha_2\left(t - \frac{a}{v_g}\right)\end{bmatrix}, \quad (74)$$

where the effective collective coupling matrix is given by

$$V_2(0) = -\frac{\Gamma}{2}\begin{bmatrix}1 & e^{ik_a a} \\ e^{ik_a a} & 1\end{bmatrix} \quad (75)$$

with a being the separation between the two emitters.

Before discussing the detailed results, let us first look at what has been changed by the effective collective coupling $V_2(0)$. First, this coupling matrix is non-Hermitian as the effects of dissipation to the photon modes are included [105]. The eigenvalues and the eigenstates of $V_2(\delta k = 0)$ are respectively given by

$$\lambda_{\pm} = -\frac{\Gamma}{2}(1 \pm \cos(k_a a)) \pm i\frac{\Gamma}{2}\sin(k_a a), \quad (76)$$

$$|\pm\rangle = \frac{1}{\sqrt{2}}(|eg\rangle \pm |ge\rangle). \quad (77)$$

The real parts of $\lambda_{\pm}$ are the collective decay rate while the imaginary parts are the energy shifts. The eigenstates of the

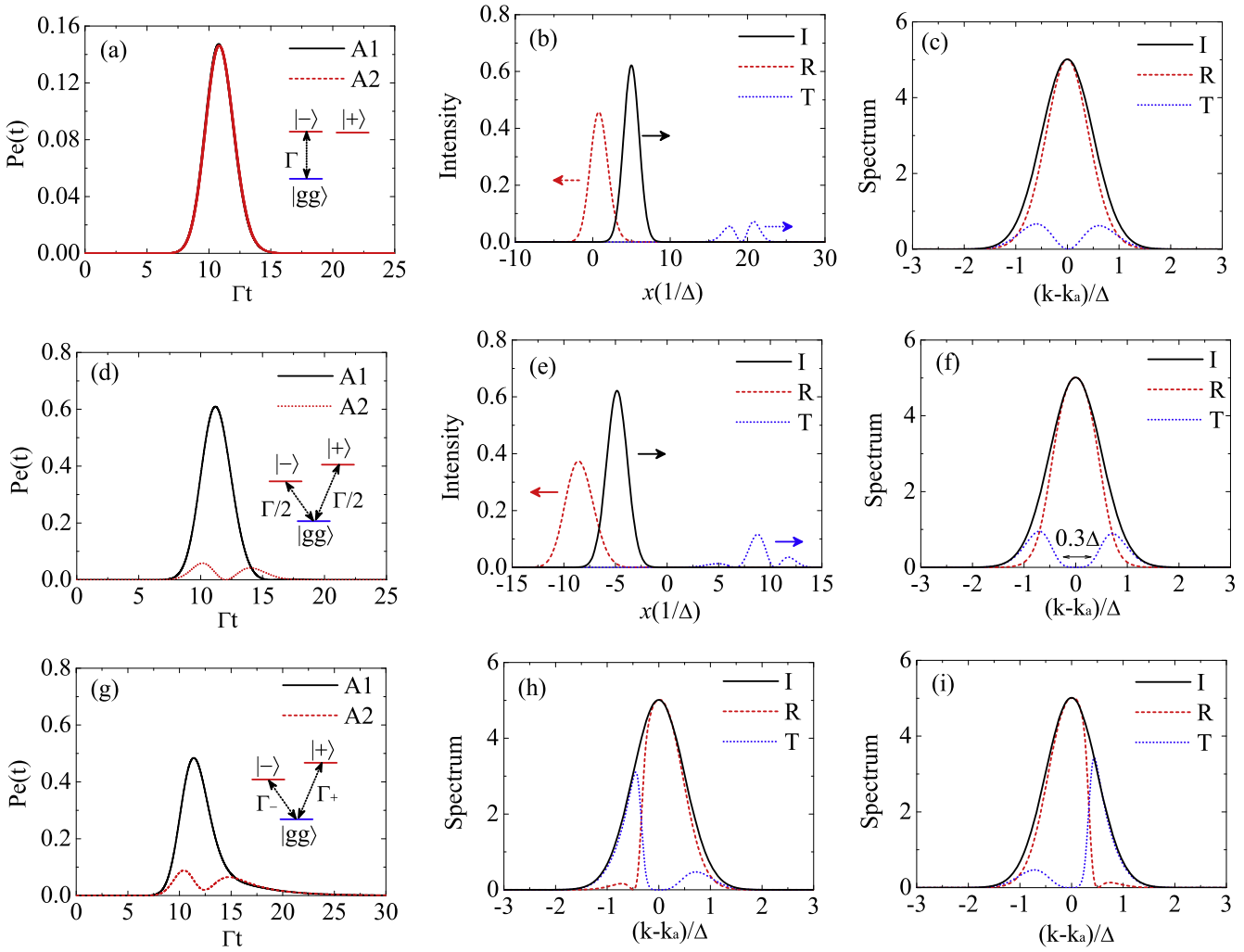

Figure 6. (a), (d) and (g) The atomic excitations (A1: atom 1 and A2: atom 2) as a function of time. When $t = 0$ the center of the input pulse is $10/\Delta$ away from the first atom. Here, A1 is for atom 1 and A2 is for atom 2. (b) and (e) The pulse shapes of the incoming (I, at $t = 6/\Gamma$), reflected (R, at $t = 20/\Gamma$) and transmitted (T, at $t = 20/\Gamma$) photon. (c), (f), (h) and (i) The spectrum (arb. units) of the incoming (I), reflected (R) and transmitted (T) photon. Parameters: $\Gamma = \Delta v_g$, (a)–(c) $a = \lambda/2$, (d)–(f) $a = \lambda/4$, (g) and (h) $a = \lambda/8$, (i) $a = 3\lambda/8$. Figure reprinted with permission from Liao *et al* (2015) [58]. Copyright 2015 by the American Physical Society.

coupling matrix are two Dicke states. By changing the emitter separation, one can tune the collective decays and the energy shifts.

The photon spectra when $t \to \infty$ are given by

$$\beta_{\delta k}^{\mathrm{R}} = \beta_{\delta k}(0)\frac{-4\delta k^2 v_g^2/\Gamma^2}{(1 - 2i\delta k v_g/\Gamma)^2 - \mathrm{e}^{2ika}}, \tag{78}$$

$$\beta_{\delta k}^{\mathrm{L}} = \beta_{\delta k}(0)\mathrm{e}^{2ikr_1}\frac{(1 + \mathrm{e}^{2ika})(1 - 2i\delta k v_g/\Gamma) - 2\mathrm{e}^{2ika}}{(1 - 2i\delta k v_g/\Gamma)^2 - \mathrm{e}^{2ika}}, \tag{79}$$

where $k = k_a + \delta k$. We can see that the reflectivity and transmissivity for each component are the same as those calculated by the Bethe ansatz shown in equations (62) and (63). In the following we compare the results for four different atomic separations, i.e., $a = \lambda/4$, $\lambda/2$, $\lambda/8$ and $3\lambda/8$.

In figures 6(a)–(c) we show the results when $a = \lambda/2$ and $\Gamma = \Delta v_g$. When $a = \lambda/2$, the eigenvalues of the coupling matrix are $\lambda_+ = 0$ and $\lambda_- = -\Gamma$. Thus, in this case the collective coupling only modifies the collective decay rates but does not shift the eigenenergy. Here we note that the antisymmetric state $\lambda_-\rangle$ is superradiant while the symmetric state $|\lambda_+\rangle$ does not couple to the waveguide modes at all. This is different from the usual case with Markov approximation due to the extra phase factor $\mathrm{e}^{\mathrm{i}\pi}$ caused by the spatial separation between the two emitters, which is similar to the timed-Dicke state [88]. Hence, the system can be prepared in the $|\lambda_-\rangle$ eigenstate where the two emitters are excited by about equal probabilities (figure 6(a)). Since only one eigenstate is coupled to the ground state, the photon pulse shape (figure 6(b)) and photon spectrum (figure 6(c)) are similar to those in the single emitter case. However, due to the enhanced collective decay rate, the reflectivity here is about 84% which is larger than that in the single emitter case.

When $a = \lambda/4$, the eigenvalues of the coupling matrix are $\lambda_\pm = -\Gamma/2 \pm \mathrm{i}\Gamma/2$. The collective interaction induces energy shifts of the eigenstates but does not modify the collective decay rates. The two eigenstates $|\lambda_\pm\rangle$ have different

energies but both of them can couple to the ground state with the same coupling strength. The excitation probabilities of the two atoms as a function of time are shown in figure 6(d) where the black solid line is the excitation of the first emitter while the red dotted line is the excitation of the second emitter. The two emitters have different excitation probabilities with the first emitter being excited with a much larger probability than the second one due to the interference between the two excitation channels. The first emitter has a maximum excitation probability larger than 50%, which is not allowed for the single emitter case, because of the constructive interference. The second emitter has much smaller excitation probability and has a dip at certain time due to the destructive interference of the two channels. The photon pulses before and after the interaction are shown in figure 6(e). The reflected pulse is similar to the incident photon pulse while the transmitted pulse has three peaks instead of two peaks as in the single atom case due to the interferences between the incident field and the remitted fields by the two emitters. The spectra are shown in figure 6(f) where we see that there is a frequency bandwidth around the resonant frequency whose transmissivity is significantly suppressed. This is similar to the photonic bandgap effect. This bandgap can be changed by tuning the coupling strength or the number of emitters.

When $a = \lambda/8$, we have $\lambda_{\pm} = -(\Gamma/2)\,[(1 \pm \sqrt{2}/2) \mp i\sqrt{2}/2]$, where both the collective decay rates and the eigenenergies are modified. The excitation probabilities as a function of time are shown in figure 6(g) where we see that the two emitters have different excitation probabilities. The second emitter experiences a probability oscillation due to the destructive interference, but the dip in between does not reach zero because of the unequal coupling strengths of the two eigenstates. The reflected and transmitted spectra are shown in figure 6(h). Both the reflected and transmitted spectra are asymmetric with most of the higher frequency components being reflected and most of the lower frequency components being transmitted. These are not difficult to be explained. The single-photon excitation states are split into two eigenstates where $|+\rangle$ has higher energy with larger coupling strength while $|-\rangle$ has lower energy with smaller coupling strength. Hence, the higher frequency components have a larger probability to be reflected which results in the asymmetric spectra. Besides, we note that there is a dip in the reflected spectrum which can be explained by the spontaneous emission cancellation between the two decay channels and it is a kind of Fano-like interference [95–98]. By adjusting the emitter separation such that $a = 3\lambda/8$, one may also reflect the lower frequency components but transmit the higher frequencies. The reflected and transmitted spectra when $a = 3\lambda/8$ is shown in figure 6(i) from which we can see that they are similar to the result of $a = \lambda/8$ but the spectra are opposite.

Quantum entanglement can also be generated in this process due to the collective interaction between the two emitters [31, 53, 58]. The concurrence of the two-emitter system is given by $C(t) = \max\{0, 2|\alpha_1(t)||\alpha_2(t)|\}$, where $C(t)$ denotes the quantum concurrence of the two-atom system

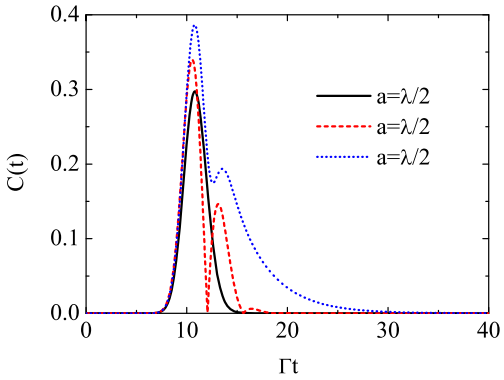

Figure 7. The concurrences as a function of time for three different atomic separations ($a = 0.5\lambda$: black solid line; $a = 0.25\lambda$: red dotted line; $a = 0.125\lambda$: blue dashed line). Parameter: $\Gamma = \Delta v_g$. Figure reprinted with permission from Liao *et al* (2015) [58]. Copyright 2015 by the American Physical Society.

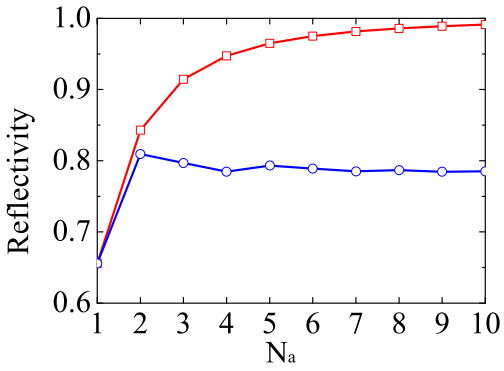

Figure 8. The reflectivity as a function of atom numbers for two atomic separations: $a = \lambda/2$ (red line with squares) and $a = \lambda/4$ (blue line with circles). Parameters: $\Gamma = \Delta v_g$. Figure reprinted with permission from Liao *et al* (2015) [58]. Copyright 2015 by the American Physical Society.

at time t [107]. The concurrences as a function of time for three different emitter separations ($a = 0.5\lambda$, 0.25λ, 0.125λ) are shown in figure 7, where we can clearly see that quantum entanglement between the two emitters can be generated. When $a = \lambda/4$ the quantum entanglement undergoes several sudden death and revival oscillations due to the interference between the two decay channels. When $a = \lambda/8$, the quantum entanglement can last much longer than the other two cases (blue dashed line) because one of its eigenstates is sub-radiant state.

We can also calculate the photon transport when there are more than two emitters [58]. When $a = \lambda/2$, only one eigenvalue of the effective coupling matrix $V_{N_a}(0)$ is non-zero and it is given by $\lambda_l = N_a\Gamma/2$. Due to this collective enhanced coupling strength, the reflectivity of the system can approach 100%. For example, when $N_a = 5$, the reflectivity can be about 96%. The reflectivity as a function of emitter number for $a = \lambda/2$ and $a = \lambda/4$ are shown in figure 8. For $a = \lambda/2$, the reflectivity can increase as the number of emitters increases (see the line with squares in figure 8). However, when $a = \lambda/4$, the reflectivity does not change significantly when the number of emitters increases (see the

line with circles in figure 8). Hence, an emitter array with emitter separation being half integer number of wavelength can be a very good mirror. For more detail results about the $N_a > 2$, please refer to [58].

5. Few photons scattered by a quantum emitter

Multiple-photon transport in a 1D waveguide QED system is a more challenging task. The two-photon problem was first addressed by Shen and Fan based on the generalized Bethe ansatz [17, 55]. The scattering eigenstates were found by first constructing the Bethe-like eigenstates and then deducing the two-photon bound state via the completeness argument. This method is not easy to be generalized to the three-photon or more scattering problem. In subsetion A, we present a method proposed by Zheng *et al* in which one can explicitly construct the n-photon scattering eigenstates [40]. In section 5.2, we show a method based on the input–output formalism to calculate the scattering matrix of few-photon transport , which is proposed by Fan *et al* [37].

5.1. Bethe-ansatz approach

For a few photons interact with a single emitter coupled to a 1D waveguide, the Hamiltonian is the same as equation (5). The photon part can be decomposed as even and odd modes where we can rewrite $a_e^\dagger(x) = [a_R^\dagger(x) + a_L^\dagger(-x)]/\sqrt{2}$ and $a_o^\dagger(x) = [a_R^\dagger(x) - a_L^\dagger(-x)]/\sqrt{2}$. The Hamiltonian can then be rewritten as $H = H_e + H_o$ with

$$H_e = -\mathrm{i}v_g\int \mathrm{d}x a_e^\dagger \frac{\partial}{\partial x}a_e(x) + (\omega_a - \mathrm{i}\gamma/2)|e\rangle\langle e| + \sqrt{2}\,g\int \mathrm{d}x\delta(x)[a_e^\dagger(x)S^- + a_e^-(x)S^+], \tag{80}$$

$$H_o = -\mathrm{i}v_g\int \mathrm{d}x a_o^\dagger \frac{\partial}{\partial x}a_o(x). \tag{81}$$

It is noted that $[H, n_e + n_a] = [H, n_o] = 0$, where $n_e = \int \mathrm{d}x a_e^\dagger a_e(x)$ is the number operator for the even modes, $n_o = \int \mathrm{d}x a_o^\dagger a_o(x)$ is the number operator for the odd modes, and n_a is the excitation number of the quantum emitter. Thus, the total numbers of excitations are conserved in both the even and the odd subspace separately. Since only the even modes can couple to the emitter, we would mainly calculate the scattering of the even modes. The odd modes can pass through without scattering.

An n-excitation state in the even subspace can be written as [40]

$$|\psi_n\rangle = \int \mathrm{d}x_1\cdots\mathrm{d}x_n f_n(x_1,\ldots,x_n)a_e^\dagger(x_1)\cdots a_e^\dagger(x_n)|0, g\rangle + \int \mathrm{d}x_1\cdots\mathrm{d}x_{n-1}e_n(x_1,\ldots,x_{n-1})a_e^\dagger(x_1)\cdots a_e^\dagger(x_{n-1})|0, e\rangle. \tag{82}$$

From the eigen-equation $H_e|\psi_n\rangle = E_n|\psi_n\rangle$ with $E_n/v_g = k_1 + k_2 + \cdots k_n$, one can obtain the following equations [40]

$$\{-\mathrm{i}v_g(\partial_{x_1}+\cdots+\partial_{x_n}) - E_n\}f_n(x_1,\ldots,x_n) + \frac{\sqrt{2}\,g}{n}[\delta(x_1)e_n(x_2,\ldots,x_n)+\cdots+\delta(x_n)e_n(x_1,\ldots,x_{n-1})] = 0, \tag{83}$$

$$\left\{-\mathrm{i}v_g(\partial_{x_1}+\cdots+\partial_{x_n}) - E_n + \omega_a - \mathrm{i}\frac{\gamma}{2}\right\}e_n(x_1,\ldots,x_{n-1}) + \sqrt{2}\,gnf_n(0, x_1,\ldots,x_{n-1}) = 0, \tag{84}$$

where $f_n(x_1,\ldots,x_n)$ can be discontinuous at $x_i = 0$, $i = 1,\ldots,n$ and we can set $f_n(0, x_1,\ldots,x_{n-1}) = [f_n(0^+, x_1,\ldots,x_n) + f_n(0^-, x_1,\ldots,x_n)]/2$.

Assuming that the incident photons are plane waves, we have

$$f_n(x_1,\ldots,x_n) = \frac{1}{n!}\sum_Q \phi_{k_1}(x_{Q_1})\cdots\phi_{k_n}(x_{Q_n}), \tag{85}$$

where $\phi_k(x) = (1/\sqrt{2\pi})\mathrm{e}^{\mathrm{i}kx}$ and Q is the permutation of the sets $[1, 2,\ldots,n]$. From this initial condition and equations (83) and (84), it is, in principle, able to solve the scattering wavefunction.

For the single photon case ($n = 1$), equations (83) and (84) become

$$(-\mathrm{i}v_g\partial_x - kv_g)f_1(x) + \sqrt{2}\,g\delta(x)e_1 = 0, \tag{86}$$

$$\left(-\mathrm{i}v_g\partial_x - kv_g + \omega_a - \mathrm{i}\frac{\gamma}{2}\right)e_1 + \sqrt{2}\,gf_1(0) = 0. \tag{87}$$

The solution is given by [40]

$$f_1(x) = \phi_k(x)[\theta(-x) + t_k\theta(x)], \tag{88}$$

$$e_1 = \frac{\mathrm{i}v_g}{2\sqrt{\pi}\,g}(t_k - 1) \tag{89}$$

with

$$t_k = \frac{2\delta kv_g - \mathrm{i}(\Gamma - \gamma)}{2\delta kv_g + \mathrm{i}(\Gamma + \gamma)} \tag{90}$$

being the transmission coefficient of the even modes and $\Gamma = 2g^2/v_g$.

For the two-photon case ($n = 2$), equations (83) and (84) become

$$[-\mathrm{i}v_g(\partial_{x_1} + \partial_{x_2}) - (k_1 + k_2)v_g]f_2(x_1, x_2) + \frac{g}{\sqrt{2}}[\delta(x_1)e_2(x_2) + \delta(x_2)e_2(x_1)] = 0, \tag{91}$$

$$[-\mathrm{i}v_g\left(\partial_{x_1} + \partial_{x_2} - (k_1 + k_2)v_g + \omega_a - \mathrm{i}\frac{\gamma}{2}\right)e_2(x_1, x_2) + 2\sqrt{2}\,gf_2(0, x) = 0 \tag{92}$$

whose solutions are given by (see the appendix in [40])

$$f_2(x_1, x_2) = \frac{1}{2}[f_{k_1}(x_1)f_{k_2}(x_2) + f_{k_1}(x_2)f_{k_2}(x_1) + B^2_{k_1,k_2}(x_1, x_2)\theta(x_1) + B^2_{k_1,k_2}(x_2, x_1)\theta(x_2)], \tag{93}$$

$$e_2(x) = \frac{\sqrt{2}\,\mathrm{i}}{g}[f_2(0^+, x) - f_2(0^-, x)], \tag{94}$$

where

$$B^2_{k_1,k_2}(x_1, x_2) = -(t_{k_1} - 1)(t_{k_2} - 1)\phi_{k_1}(x_2)\phi_{k_2}(x_2) \times \mathrm{e}^{(-\Gamma/2-\mathrm{i}\omega_a)|x_2-x_1|}\theta(x_2 - x_1) \tag{95}$$

is the two-body photon bound-state term [17, 40, 55]. This photon bound-state is occurred when the two photons interact with the quantum emitter at the same time. In this photon bound-state, the two photons tend to propagate together. The formation of bound state can be explained by the stimulated emission, i.e., the first photon excites the emitter and then the second photon stimulates the emission of the emitter and therefore the two photons after the scattering tend to bound together.

The calculations for $N > 2$ photons are much complicated. For details, please refer to [40].

5.2. Input–output formalism

In this subsection, we show the calculation of scattering matrix of few-photon transport via the input–output formalism [37, 101, 102]. For the two-photon transport, the scattering matrix is given by [37]

$$\langle\tilde{p}_1\tilde{p}_2|S|\tilde{k}_1\tilde{k}_2\rangle = \langle 0|a_{\mathrm{out}}(\tilde{p}_1)a_{\mathrm{out}}(\tilde{p}_2)a^{\dagger}_{\mathrm{in}}(\tilde{k}_1)a^{\dagger}_{\mathrm{in}}(\tilde{k}_2)|0\rangle. \tag{96}$$

By inserting the identity $\int \mathrm{d}k|\tilde{k}^-\rangle\langle\tilde{k}^-|$ between $a_{\mathrm{out}}(\tilde{p}_1)$ and $a_{\mathrm{out}}(\tilde{p}_2)$, and using the Fourier transformation of equation (23), we get

$$\begin{aligned}
&\langle\tilde{p}_1\tilde{p}_2|S|\tilde{k}_1\tilde{k}_2\rangle \\
&= t_{\tilde{p}_1}\langle\tilde{p}_1^-|a_{\mathrm{out}}(\tilde{p}_2)a^{\dagger}_{\mathrm{in}}(\tilde{k}_1)a^{\dagger}_{\mathrm{in}}(\tilde{k}_2)|0\rangle \\
&= t_{\tilde{p}_1}\langle\tilde{p}_1^-|[a_{\mathrm{in}}(\tilde{p}_2) - \mathrm{i}\Gamma\sigma^-(\tilde{p}_2)]a^{\dagger}_{\mathrm{in}}(\tilde{k}_1)a^{\dagger}_{\mathrm{in}}(\tilde{k}_2)|0\rangle \\
&= t_{\tilde{p}_1}\delta(\tilde{p}_1 - \tilde{k}_1)\delta(\tilde{p}_2 - \tilde{k}_2) + t_{\tilde{p}_1}\delta(\tilde{p}_1 - \tilde{k}_2)\delta(\tilde{p}_2 - \tilde{k}_1) \\
&\quad - \mathrm{i}\sqrt{\Gamma}\,t_{\tilde{p}_1}\langle\tilde{p}_1^-|\sigma^-(\tilde{p}_2)|\tilde{k}_1^-\tilde{k}_2^-\rangle,
\end{aligned} \tag{97}$$

where $t_{\tilde{k}}$ is defined by equation (33). Hence, to determine the scattering matrix, we can first calculate $\langle\tilde{p}_1^-|\sigma^-(t)|\tilde{k}_1^-\tilde{k}_2^-\rangle$ and then calculate its Fourier transformation.

From equation (22), we have the differential equation

$$\frac{\mathrm{d}}{\mathrm{d}t}\langle\tilde{p}_1^-|\sigma^-(t)|\tilde{k}_1^-\tilde{k}_2^-\rangle = \mathrm{i}\sqrt{\Gamma}\,\langle\tilde{p}_1^-|\sigma_z(t)a_{\mathrm{in}}(t)|\tilde{k}_1^-\tilde{k}_2^-\rangle - \left(\mathrm{i}\Omega + \frac{\Gamma}{2}\right)\langle\tilde{p}_1^-|\sigma^-(t)|\tilde{k}_1^-\tilde{k}_2^-\rangle, \tag{98}$$

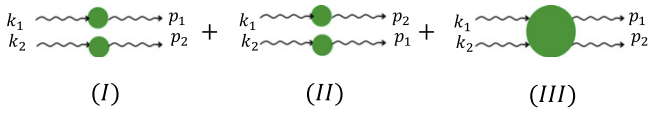

Figure 9. The diagrammatic representation of the two-photon scattering matrix.

where the first term can be calculated to be

$$\frac{\mathrm{i}\sqrt{\Gamma}}{\sqrt{2\pi}}[\langle\tilde{p}_1^-|\sigma_z(t)|\tilde{k}_1^-\rangle\mathrm{e}^{-\mathrm{i}k_2 t} + \langle\tilde{p}_1^-|\sigma_z(t)|\tilde{k}_2^-\rangle\mathrm{e}^{-\mathrm{i}\tilde{k}_1 t}]$$

with

$$\begin{aligned}
\langle\tilde{p}^-|\sigma_z(t)|\tilde{k}^-\rangle &= \langle\tilde{p}^-|(2\sigma_+\sigma_- - 1)|\tilde{k}^-\rangle \\
&= 2\langle\tilde{p}^-|\sigma_+|0\rangle\langle 0|\sigma_-|\tilde{k}^-\rangle - \delta(\tilde{k} - \tilde{p}) \\
&= \frac{1}{\pi}\mathrm{e}^{-\mathrm{i}(\tilde{k}-\tilde{p})t}s^*_{\tilde{p}}s_{\tilde{k}} - \delta(\tilde{k} - \tilde{p}).
\end{aligned} \tag{99}$$

On integrating equation (98) one can get

$$\begin{aligned}
&\langle\tilde{p}_1^-|\sigma^-(t)|\tilde{k}_1^-\tilde{k}_2^-\rangle \\
&= -\frac{1}{\sqrt{2\pi}}\left[\frac{1}{\pi}s_{\tilde{k}_1+\tilde{k}_2-\tilde{p}_1}s^*_{\tilde{p}_1}(s_{\tilde{k}_1} + s_{\tilde{k}_2})\mathrm{e}^{-\mathrm{i}(\tilde{k}_1+\tilde{k}_2-\tilde{p}_1)t}\right. \\
&\quad \left. + \delta(\tilde{k}_2 - \tilde{p}_1)s_{\tilde{k}_1}\mathrm{e}^{\mathrm{i}k_1 t} + \delta(\tilde{k}_1 - \tilde{p}_1)s_{\tilde{k}_2}\mathrm{e}^{-\mathrm{i}\tilde{k}_2 t}\right],
\end{aligned} \tag{100}$$

where $s_{\tilde{k}}$ is given by equation (31). By performing the Fourier transformation of equation (100), we have

$$\begin{aligned}
&\langle\tilde{p}_1^-|\sigma^-(\tilde{p}_2)|\tilde{k}_1^-\tilde{k}_2^-\rangle \\
&= -\frac{1}{\pi}\delta(\tilde{k}_1 + \tilde{k}_2 - \tilde{p}_1 - \tilde{p}_2)s_{\tilde{p}_2}s^*_{\tilde{p}_1}(s_{\tilde{k}_1} + s_{\tilde{k}_2}) \\
&\quad + \delta(\tilde{k}_2 - \tilde{p}_1)\delta(\tilde{k}_1 - \tilde{p}_2)s_{\tilde{k}_1} \\
&\quad + \delta(\tilde{k}_1 - \tilde{p}_1)\delta(\tilde{k}_2 - \tilde{p}_2)s_{\tilde{k}_2}].
\end{aligned} \tag{101}$$

On inserting equations (101) into (96), one can obtain the scattering matrix [37]

$$\begin{aligned}
&\langle\tilde{p}_1\tilde{p}_2|S|\tilde{k}_1\tilde{k}_2\rangle \\
&= t_{\tilde{k}_1}t_{\tilde{k}_2}[\delta(\tilde{k}_1 - \tilde{p}_1)\delta(\tilde{k}_2 - \tilde{p}_2) + \delta(\tilde{k}_2 - \tilde{p}_1)\delta(\tilde{k}_1 - \tilde{p}_2)] \\
&\quad + \mathrm{i}\frac{\Gamma}{\pi}\delta(\tilde{k}_1 + \tilde{k}_2 - \tilde{p}_1 - \tilde{p}_2)s_{\tilde{p}_1}s_{\tilde{p}_2}(s_{\tilde{k}_1} + s_{\tilde{k}_2})
\end{aligned} \tag{102}$$

which is consistent with the previous results based on the Bethe ansatz [40, 55, 56], and the LSZ formalism in quantum field theory [30, 44]. The diagrammatic representation of the two-photon scattering matrix is shown in figure 9 where the three processes correspond to the three terms shown in equation (102). In addition to the Fock state input, the method here may be also applied to the coherent state input [37].

6. Multiple photons scattered by a local system

In general, the calculation of multiple photons interacting with multiple quantum emitters is very complicated. Here we briefly show a systematic treatment of N-photon transport in a 1D waveguide coupled to a local system via the input–output formalism proposed by Xu and Fan [42].

The Hamiltonian of a single-mode waveguide coupled to a local system which may consist of multiple quantum emitters may be written as [42]

$$H = H_s + \int dk k a_k^\dagger a_k + g \int dk (a_k^\dagger b + a_k b^\dagger), \quad (103)$$

where H_s is the Hamiltonian of the local system, $a_k (a_k^\dagger)$ is the annihilation (creation) operator of the guided photon, and $b(b^\dagger)$ is one of several possible system operators that couple to the guided photon modes with coupling strength being g. In the input–output formalism, the N-photon scattering matrix can be written as [42]

$$S_{p_1 \cdots p_N; k_1 \cdots k_N} = FT \left\{ \langle 0 | \prod_{i=1}^{N} a_{out}(t_i') \prod_{j=1}^{N} a_{in}^\dagger(t_j) | 0 \rangle \right\}, \quad (104)$$

where FT denotes the Fourier transformation and $a_{in}(t)$ and $a_{out}(t)$ satisfy the relation [101, 102] $a_{out}(t) = a_{in}(t) - i\sqrt{\Gamma} b(t)$, where $\Gamma = 2\pi g^2 / v_g$. Similar to the procedures using the input–output formalism shown in the previous sections, one can derive the scattering matrix from the Heisenberg equations and get [42]

$$S_{p_1 \cdots p_N; k_1 \cdots k_N} = \sum_{M=0}^{N} \sum_{B_M, D_M} G(p_{B_M}; k_{D_M}) \sum_P \prod_{\substack{m_1 \in B_M^c \\ m_2 \in D_M^c}} \delta(p_{m_1} - k_{m_2}), \quad (105)$$

where B_M and D_M are two subsets of $\{1, \ldots, N\}$ with M elements, B_M^c and D_M^c are the complementary subsets of B_M and D_M respectively, and $G(p_{B_M}; k_{D_M}) = FT[G(t_1' \cdots t_M'; t_1' \cdots t_M')]$ is the Fourier transformation of a $2M$-point Green's function of the local system with $G(t_1' \cdots t_M'; t_1' \cdots t_M')$ being given by $(-\Gamma)^M \langle 0 | T[b(t_1') \cdots b(t_M') b^\dagger(t_1) \cdots b^\dagger(t_M)] | 0 \rangle$. It is shown that this Green's function can be calculated using the effective Hamiltonian of the local system. For details, please refer to section 6 in [42].

In addition to the input–output theory, the multiphoton scattering with multiple two-level atoms located in a small region coupled to a 1D waveguide has also being studied based on the theory of integrable quantum systems [56]. A general formalism to calculate the scattering matrix of an arbitrary multi-particle wavepacket transport in a 1D multi-mode chiral waveguide coupled to an ensemble of distributed emitters has also been derived based on a direct and resummation of a diagrammatic series of multi-particle scattering matrix [57]. This method has been applied for several problems such as the tunable nonlinear Hong–Ou–Mandel interferometer based on two-photon scattering coupled to a single-mode cavity and two waveguides [108], and the exact solution of the scattering of two photons from two distant qubits [109]. For more details, please refer to [57].

7. Summary and outlook

In this article, we summarize the approaches to calculate photon transport in a 1D waveguide coupled to a system of quantum emitters. For static solution, we illustrate the methods based on the Bethe anstaz and the input–output formalism which give the same results. It is shown that a resonant frequency can be completely reflected back by a quantum emitter in a 1D waveguide which may be used as a perfect mirror. We also derive a time-dependent dynamical theory to calculate the single-photon transport interacting with multiple quantum emitters which allows us to calculate the real-time evolution of the whole system. It is shown that the reflectivity of a single photon pulse with finite bandwidth can approach 100% if the coupling strength or the collective coupling strength is much larger than the photon bandwidth. The spectrum of the reflected and transmitted photon can also be significantly different from the single atom case. Many interesting physical phenomena can occur in this system such as the photonic bandgap effects, quantum entanglement generation, Fano-like interference, and superradiant effects.

The waveguide QED system may find important applications in quantum device and quantum information technology. For instance, the 1D waveguide QED system may serve as a single photon source, single photon mirror, single photon frequency filter, single photon modulation, and single photon frequency converter. Moreover, a single-photon transistor using nanoscale 1D surface plasmons, photon-photon π-phase gate in a 1D waveguide, and a single-photon quantum router with multiple output ports have also been proposed. Due to these possible applications, waveguide-QED system is still a very interesting area that requires further extensive study. Here, we mention several possible issues that can be addressed in the future. (a) One may extend the dynamical solution to multi-photon cases from which one can either theoretical or numerical calculate the real-time evolution of the multi-photon system which may be useful to design a multiple-photon quantum gate and study many-body physics. (b) One may also generalize the calculations to multiple waveguide system which may find important applications for quantum computation and quantum network. (c) Waveguide-based quantum communication or teleportation are also interesting topics to be studied. (d) One may also study the hybrid system that combines a dielectric waveguide and a surface plasmon medium such as graphene to extend the controllability.

Acknowledgments

This work is supported by a grant from the Qatar National Research Fund (QNRF) under the NPRP project 7-210-1-032.

References

[1] Raimond J M, Brune M and Haroche S 2007 *Rev. Mod. Phys.* **73** 565
[2] Pelton M, Santori C, Vučković J, Zhang B, Solomon G S, Plant J and Yamamoto Y 2002 *Phys. Rev. Lett.* **89** 233602
[3] Wilk T, Webster S C, Kuhn A and Rempe G 2007 *Science* **317** 488

[4] Chang D E, Sørensen A S, Demler E A and Lukin M D 2007 *Nat. Phys.* **3** 807
[5] Hwang J, Pototschnig M, Lettow R, Zumofen G, Renn A, Götzinger S and Sandoghdar V 2009 *Nature* **460** 76
[6] Bermel P, Rodriguez A, Johnson S G, Joannopoulos J D and Soljaî¡ić M 2006 *Phys. Rev.* A **74** 043818
[7] O'Brien J L, Furusawa A and Vučković J 2009 *Nat. Photon.* **3** 687
[8] Purcell E M 1946 *Phys. Rev.* **69** 674
[9] Walther H, Varcoe B T H, Englert B G and Becker T 2006 *Rep. Prog. Phys.* **69** 1325
[10] Pellizzari T, Gardiner S A, Cirac J I and Zoller P 1995 *Phys. Rev. Lett.* **75** 3788
[11] Yoshie T, Scherer A, Hendrickson J, Khitrova G, Gibbs H M, Rupper G, Ell C, Shchekin O B and Deppe D G 2004 *Nature* **432** 200
[12] Turchette Q A, Thompson R J and Kimble H J 1995 *Appl. Phys.* B **60** S1
[13] Leistikow M D, Mosk A P, Yeganegi E, Huisman S R, Lagendijk A and Vos W L 2011 *Phys. Rev. Lett.* **107** 193903
[14] Noda S, Fujita M and Asano T 2007 *Nat. Photon.* **1** 449
[15] Shen J-T and Fan S 2005 *Opt. Lett* **30** 2001
[16] Shen J-T and Fan S 2005 *Phys. Rev. Lett.* **95** 213001
[17] Shen J-T and Fan S 2007 *Phys. Rev. Lett.* **98** 153003
[18] Roy D 2011 *Phys. Rev. Lett.* **106** 053601
[19] Tsoi T S and Law C K 2009 *Phys. Rev.* A **80** 033823
[20] Wang Z H, Zhou L, Li Y and Sun C P 2014 *Phys. Rev.* A **89** 053813
[21] Fang Y-L L, Zheng H and Baranger H U 2014 *EPJ Quantum Technol.* **1** 3
[22] Fang Y-L L and Baranger H U 2015 *Phys. Rev.* A **91** 053845
[23] Rephaeli E, Shen J-T and Fan S 2010 *Phys. Rev.* A **82** 033804
[24] Chen Y, Wubs M, Mørk J and Koenderink A F 2011 *New J. Phys.* **13** 103010
[25] Tsoi T S and Law C K 2008 *Phys. Rev.* A **78** 063832
[26] Roy D 2013 *Sci. Rep.* **3** 2337
[27] Shen J-T and Fan S 2009 *Phys. Rev.* A **79** 023837
[28] Zhou L, Gong Z R, Liu Y-X, Sun C P and Nori F 2008 *Phys. Rev. Lett* **101** 100501
[29] Rephaeli E and Fan S 2012 *Phys. Rev. Lett.* **108** 143602
[30] Longo P, Schmittechert P and Busch K 2010 *Phys. Rev. Lett.* **104** 023602
[31] Zheng H, Gauthier D J and Baranger H U 2011 *Phys. Rev. Lett.* **107** 023601
[32] Zheng H and Baranger H U 2013 *Phys. Rev. Lett.* **111** 090502
[33] Liao J Q and Law C K 2010 *Phys. Rev.* A **82** 053836
[34] Huang J F, Shi T, Sun C P and Nori F 2013 *Phys. Rev.* A **88** 013836
[35] Witthaut D and Sorensen A S 2010 *New J. Phys.* **12** 043052
[36] Li Q, Zhou L and Sun C P 2013 *Phys. Rev.* A **89** 063810
[37] Fan S, Kocabas S E and Shen J-T 2010 *Phys. Rev.* A **82** 063821
[38] Lalumière K, Sanders B C, van Loo A F, Fedorov A, Wallraff A and Blais A 2013 *Phys. Rev.* A **88** 043806
[39] Ciccarello F, Browne D E, Kwek L C, Schomerus H, Zarcone M and Bose S 2012 *Phys. Rev.* A **85** 050305(R)
[40] Zheng H, Gauthier D J and Baranger H U 2010 *Phys. Rev.* A **82** 063816
[41] Shi T and Sun C P 2009 *Phys. Rev.* B **79** 205111
[42] Xu S and Fan S 2015 *Phys. Rev.* A **91** 043845
[43] Baragiola B Q, Cook R L, Brańczyk A M and Combes J 2012 *Phys. Rev.* A **86** 013811
[44] Shi T, Fan S and Sun C P 2011 *Phys. Rev.* A **84** 063803
[45] Hach E E III, Elshaari A W and Preble S F 2010 *Phys. Rev.* A **82** 063839
[46] Bradford M, Obi K C and Shen J-T 2012 *Phys. Rev. Lett.* **108** 103902
[47] Menon V M, Tong W, Xia F, Li C and Forrest S R 2004 *Opt. Lett.* **29** 513
[48] Yan W-B, Huang J-F and Fan H 2013 *Sci. Rep.* **3** 3555
[49] Dong H, Gong Z R, Ian H, Zhou L and Sun C P 2009 *Phys. Rev.* A **79** 063847
[50] Bradford M and Shen J-T 2012 *Phys. Rev.* A **85** 043814
[51] Li T Y, Huang J F and Law C K 2015 *Phys. Rev.* A **91** 043834
[52] Shen Y, Bradford M and Shen J-T 2011 *Phys. Rev. Lett.* **107** 173902
[53] González-Tudela A and Porras D 2013 *Phys. Rev. Lett.* **110** 080502
[54] Yan W-B and Fan H 2014 *Sci. Rep.* **4** 4820
[55] Shen J-T and Fan S 2007 *Phys. Rev.* A **76** 062709
[56] Yudson V I and Reineker P 2008 *Phys. Rev.* A **78** 052713
[57] Pletyukhov M and Gritsev V 2012 *New J. Phys.* **14** 095028
[58] Liao Z, Zeng X, Zhu S-Y and Zubairy M S 2015 *Phys. Rev.* A **92** 023806
[59] Dayan B, Parkins A S, Aoki T, Ostby E P, Vahala K J and Kimble H J 2013 *Science* **319** 1062
[60] Vetsch E, Reitz D, Sague E, Schmidt R, Dawkins S T and Rauschenbeutel A 2010 *Phys. Rev. Lett.* **104** 203603
[61] Akimov A V, Mukherjee A, Yu C L, Chang D E, Zibrov A S, Hemmer P R, Park H and Lukin M D 2007 *Nature* **450** 402
[62] Bajcsy M, Hofferberth S, Balic V, Peyronel T, Hafezi M, Zibrov A S, Vuletic V and Lukin M D 2009 *Phys. Rev. Lett.* **102** 203902
[63] Babinec T M, Hausmann J M, Khan M, Zhang Y, Maze J R, Hemmer P R and Lonî¡ar M 2010 *Nat. Nanotechnol.* **5** 195
[64] Claudon J, Bleuse J, Malik N S, Bazin M, Jaffrennou P, Gregersen N, Sauvan C, Lalanne P and Gérard J-M 2010 *Nat. Nanotechnol.* **5** 195
[65] Astafiev O V, Abdumalikov A A Jr., Pashkin Yu A, Yamamoto T, Inomata K, Nakamura Y and Tsai J S 2010 *Science* **327** 840
[66] Astafiev O V, Abdumalikov A A Jr, Zagoskin A M, Pashkin Yu A, Inomata K, Nakamura Y and Tsai J S 2010 *Phys. Rev. Lett.* **104** 183603
[67] Bleuse J, Claudon J, Creasey M, Malik N S, Gérard J-M, Maksymov I, Hugonin J-P and Lalanne P 2011 *Phys. Rev. Lett.* **106** 103601
[68] Laucht A *et al* 2012 *Phys. Rev.* X **2** 011014
[69] Yu S P, Hood J D, Muniz J A, Martin M J, Norte R, Hung C L, Meenehan S M, Cohen J D, Oskar P and Kimble H J 2014 *Appl. Phys. Lett.* **104** 111103
[70] Gonzalez-Tudela A, Hung C-L, Chang D E, Cirac J I and Kimble H J 2015 *Nat. Photon.* **9** 320
[71] Aoki T, Parkins A S, Alton D J, Regal C A, Dayan B, Ostby E, Vahala K J and Kimble H J 2009 *Phys. Rev. Lett.* **102** 083601
[72] Englund D, Faraon A, Zhang B, Yamamoto Y and Vučković J 2007 *Opt. Exp.* **15** 5550
[73] Wallraff A, Schuster D I, Blais A, Frunzio L, Huang R-S, Majer J, Kumar S, Girvin S M and Schoelkopf R J 2004 *Nature* **431** 162
[74] Abdumalikov A A Jr, Astafiev O, Zagoskin A M, Pashkin Yu A, Nakamura Y and Tsai J S 2015 *Phys. Rev.* A **91** 043834
[75] Hoi I-C, Wilson C M, Johansson G, Palomaki T, Peropadre B and Delsing P 2011 *Phys. Rev. Lett.* **107** 073601
[76] Hoi I-C, Palomaki T, Lindkvist J, Johansson G, Delsing P and Wilson C M 2012 *Phys. Rev. Lett.* **108** 263601
[77] van Loo A F, Fedorov A, Lalumiére K, Sanders B C, Blais A and Wallraff A 2013 *Science* **342** 1494
[78] Taylor J R 1972 *Scattering Theory: The Quantum Theory on Nonrelativistic Collisions* (New York: Wiley)
[79] Dicke R H 1954 *Phys. Rev.* **93** 99
[80] MacGillivray J and Feld M 1976 *Phys. Rev.* A **14** 1169
[81] Gross M and Haroche S 1982 *Phys. Rep.* **93** 301

[82] Benedict M G, Ermolaev A M, Malyshev V A, Sokolov I V and Trifonov E D 1996 *Super-Radiance Multiatomic Coherent Emission* (New York: Taylor and Francis)
[83] Skribanowitz N, Herman I P, MacGillivray J C and Feld M S 1973 *Phys. Rev. Lett.* **30** 309
[84] Scully M O and Svidzinsky A A 2009 *Science* **325** 1510
[85] Svidzinsky A A, Chang J-T and Scully M O 2008 *Phys. Rev. Lett.* **100** 160504
[86] Svidzinsky A A, Chang J-T and Scully M O 2010 *Phys. Rev.* A **81** 053821
[87] Röhlsberger R, Schlage K, Sahoo B, Couet S and Rüffer S S 2010 *Science* **328** 1248
[88] Scully M O, Fry E S, Raymond Ooi C H and Wódkiewicz K 2006 *Phys. Rev. Lett.* **96** 010501
[89] Liao Z and Zubairy M S 2014 *Phys. Rev.* A **90** 053805
[90] Mewton C J and Ficek Z 2007 *J. Phys. B: At. Mol. Opt. Phys.* **40** S181
[91] Zoubi H 2012 *Eur. Phys. Lett.* **100** 24002
[92] Le Kien F, Dutta Gupta S, Nayak K P and Hakuta K 2005 *Phys. Rev.* A **72** 063815
[93] Zheng H and Baranger H U 2013 *Phys. Rev. Lett.* **110** 113601
[94] Das S, Agarwal G S and Scully M O 2008 *Phys. Rev. Lett.* **101** 153601
[95] Fano U 1961 *Phys. Rev.* **124** 1866
[96] Zhu S-Y and Scully M O 1996 *Phys. Rev. Lett.* **76** 388
[97] Fan S and Joannopoulos J D 2002 *Phys. Rev.* B **65** 235112
[98] Khanikaev A B, Wu C and Shvets G 2013 *Nanophotonics* **2** 247
[99] Tiecke T G, Thompson J D, de Leon N P, Liu L R, Vuletić V and Lukin M D 2014 *Nature* **508** 241
[100] Scully M O and Zubairy M S 2001 *Quantum Optics* (New York: Cambridge University Press)
[101] Collett M J and Gardiner C W 1984 *Phys. Rev.* A **30** 1386
[102] Gardiner C W and Collett M J 1985 *Phys. Rev.* A **31** 3761
[103] Kunz K S and Luebbers R J 2000 *The Finite Difference Time Domain Method for Electromagnetics* (Boca Raton, FL: CRC Press)
[104] Kolchin P, Belthangady C, Du S, Yin G Y and Harris S E 2008 *Phys. Rev. Lett.* **101** 103601
[105] Rau A R P and Wendell R A 2002 *Phys. Rev. Lett.* **89** 220405
[106] Bendickson J M, Dowling J P and Scalora M 1996 *Phys. Rev.* E **53** 4107
[107] Hill S and Wootters W K 1997 *Phys. Rev. Lett.* **78** 5022
[108] Oehri D, Pletyukhov M, Gritsev V, Blatter G and Schmidt S 2015 *Phys. Rev.* A **91** 033816
[109] Laakso M and Pletyukhov M 2014 *Phys. Rev. Lett.* **113** 183601